REVIEW

The molecular structures of starch components and their contribution to the architecture of starch granules: A comprehensive review

Serge Pérez[1] *and Eric Bertoft*[2]

[1] European Synchrotron Radiation Facility, Grenoble, France
[2] Department of Food Science, Swedish University of Agricultural Sciences, Uppsala, Sweden

Received: January 22, 2010
Revised: March 17, 2010
Accepted: March 18, 2010

Recent developments in methods and instrumentation have contributed to major advances in our understanding of the fine structure of amylose and amylopectin. The structure of the starch granule slowly unravels with new insight into key structural features. Following a brief presentation of the structural features common to all starches, the most recent findings for the structure of amylose and amylopectin are reported. The organization of different types of chains in amylopectin is discussed with a critical review of the 'cluster' model leading to the presentation of alternative models. The locations of molecular components in the starch granule are described according to a progress structural order. The description of the crystalline components is followed by a presentation of their supramolecular arrangements. The crystalline components comprise platelet nanocrystals which have already been identified and characterized, and other less well characterized 'blocklet components'. The location and state of amylose within the granule is also presented. This comprehensive review aims at distinguishing between those structural features that have received widespread acceptance and those that are still under debate, with the ambition of being educational and to provide stimulation for further fundamental investigation into the starch granule as a macromolecular assembly.

Keywords:
3-D structures / Amylopectin / Amylose / Blocklets / Starch Granules

1 Introduction

Starch is produced by green plants for energy storage over long periods. It is synthesized in a granular form in special organelles, plastids, as two principles types. In chloroplasts a temporary storage form is produced during photosynthesis, whereas long-time storage starch is produced in amyloplasts. Starch granules are mainly found in seeds, roots and tubers, as well as in stems, leaves, fruits and even pollen. Grain seeds, such as maize kernels, contain up to 75% of starch. Biosynthesis of starch granules is initiated at the hilum, and the granule grows by apposition. The granules occur in all shapes and sizes (spheres, ellipsoids, polygon, platelets and irregular tubules). They have diameters ranging from around 0.1 to 200 μm depending on their botanical origin [1–5]. Generally the difference in external morphology is sufficient to allow unambiguous characterization of the botanical origin, throughout optical microscopy. Starch granules are densely packed with semi-crystalline structures, the crystallinity varying from 15 to 45%, the density being about 1.5 g/cm^3. In the granular form, starch can be easily isolated by gravity, sedimentation, centrifugation and filtration. It can be subjected to various chemical,

Correspondence: Serge Pérez, European Synchrotron Radiation Facility, 6 rue Jules Horowitz, BP 200, F-38043 Grenoble Cedex 09, France.
E-mail: serge.perez@esrf.eu
Fax: +33-476-88-21-60

Abbreviations: β-LD, β-limit dextrins; **AFM,** atomic force microscopy; **CL,** chain length; **DB,** degree of branching; **DP,** degree of polymerization; **GWD,** glucan water dikinase; **GPC,** gel-permeation chromatography; **HPAEC,** anion exchange chromatography; **IB-CL,** interblock chain length; **IB-S,** interblock segment; **ICL,** internal chain length; **IC-S,** intercluster segment; **SAXS,** Small angle X-ray scattering; **SEM,** scanning electron microscopy; **SR,** synchrotron radiation; **TEM,** transmission electron microscopy; **WAXS,** wide angle X-ray scattering.

physical and enzymatic modifications with subsequent washing and processing.

Most of the native starch granules exhibit a Maltese cross when observed under polarized light [3]. The positive birefringence indicates a radial orientation of the principle axis of the crystallites. However, birefringence remains unchanged on both polar and equatorial sections of elongated starch granules, indicating that crystallites are extremely small and exhibit multiple orientations, which interferes during observations. Native granules yield X-ray diffraction patterns of low quality, as the bulk of the starch polymers are in an amorphous state (70% on average).

Starch is a biopolymer and consists of two major components: amylose and amylopectin. Amylose that builds up to 15–35% of the granules in most plants, is a primarily linear polysaccharide with α-(1–4)-linked D-glucose units. Some amylose molecules, particularly those of large molecular weight may have up to ten or more branches [6]. Amylopectin, is a highly branched molecule, with α-(1–4)-linked D-glucose backbones and exhibits about 5% of α-(1–6)-linked branches, which have a profound effect on the physical and biological properties (Fig. 1).

Amylose and amylopectin have indeed different properties. Amylose has a high tendency to retrograde and produce tough gels and strong films. Amylopectin, dispersed in water, is more stable and produces soft gels and weak films. Entanglements between amylose and amylopectin, along with the presence of phospholipids and lipids, have also significant effects on physical properties. In addition to amylose and amylopectin, some starches, notably genetically modified starches with increased amylose content, contain polyglucans with structures that apparently are intermediate to the major components. For example, phytoglycogen is found in certain varieties of starch, such as the sugary mutant of maize starch. Other minor components, such as phosphate monoester derivatives and phospholipids [7] although occurring at low concentrations, can drastically affect the properties of starch pastes and gels. This is particularly true for potato starch that consists of up to 0.09% phosphate derivatives and display unique properties that are attributed to the charge repelling between the covalently attached phosphate groups. Recent advances in the elucidation of the different levels of structure and architecture of starch granules are reviewed below. Readers are encouraged to refer to previous review chapters [8, 9] for earlier work in starch organization, and appreciate the progresses made over the last two decades to deciphering the complexity of the granule.

2 General features of the starch granules

2.1 Granule shapes, sizes and distributions

Starches isolated from different botanical sources show characteristic granule morphology [3, 10]. Most starch granules are produced individually in separate amyloplasts. However, there are cases where more than one granule is produced simultaneously in a single amyloplast, consequently they are more difficult to separate. These examples of compound starches are found in rice, waxy rice, oats and wrinkled peas. As seen from Fig. 2, starch granules vary in shape (spherical, oval, polygonal, lenticular, elongated, kidney shapes, *etc*.).

There exists a direct correlation between the amylose content and some morphological traits. The greater the amylose content, the greater the number of filamentous granules is found in the maize starch. Diameters of starch granules vary from submicrons to 100 μm (Table 1).

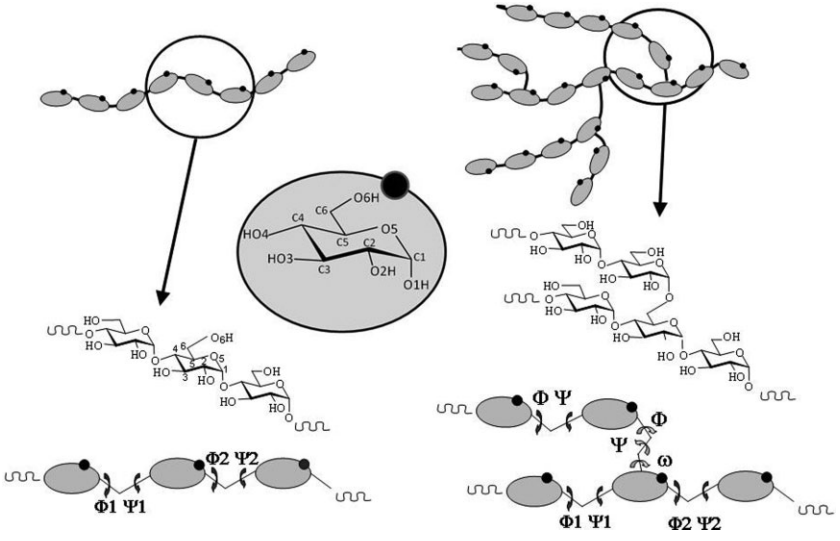

Figure 1. Basic structural motifs of amylose and amylopectin, along with the labelling of the atoms and torsion angles. Extension of the basic motifs to macromolecular structures.

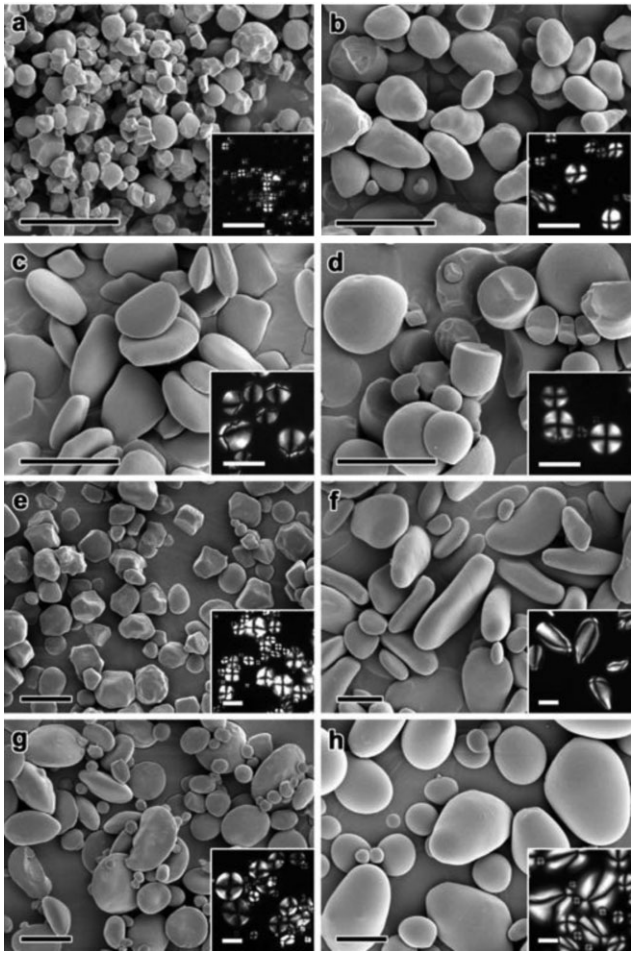

Figure 2. Scanning electron microscopy (SEM) and polarized light optical microscopy (insets) images of native starch granules from various cultivars: (a) taro; (b) chestnut; (c) ginger; (d) manioc; (e) corn; (f) green banana; (g) wheat and (h) potato. Scale bars in all images: 20 μm (micrographs: courtesy of D. Dupeyre & J. L. Putaux, CERMAV).

Table 1. Dimensions of starch granules

Origin	Dimensions (microns)
Small wheat granules	2–3
Large wheat granules	22–36
Potato starch	15–75
Canna starch	up to 100
Maize starch	5–20
Rice starch	3–8
Legume starch	10–45
Amaranth; cow cockle; pig weed,	Submicrons – 2 μm
Taro, Quinoa	Submicrons – 2 μm

2.2 The common structural features

At the lowest level of structure, most starch granules are made up of alternating amorphous and semi-crystalline shells which are between 100 and 400 nm thick [8, 11–13]. These structures are termed 'growth rings' (Fig. 3). The radial organization of the amylopectin within such structures is thought to cause optical polarization, since the visible optical polarization is in the order of the wavelength of the visible light (100–1000 nm). At a higher level of molecular order, X-ray diffraction investigations [14–16] indicate a periodicity of about 9–10 nm within the granule. The periodicity is interpreted as being due to crystalline and amorphous lamellae found within the semi-crystalline shells. These would be formed by clusters of side chains, branching off from the radially arranged amylopectin molecules. These would appear to be a universal feature in the structure of starch, independent of botanical source. Furthermore, it suggests a common mechanism for starch deposition [17]. Good quality powder diffraction patterns can be obtained from starch powder treated by mild acid hydrolysis to remove amorphous materials. These patterns can be used to identify several allomorphs [18] and to group most starches conveniently according to their physical properties. Generally, most cereal starches give the so-called A-type pattern, some tubers (such as potato and lesser yam), rhizomes (*e.g*. canna), and cereal starches rich in amylose yield the B-pattern; legume starches generally have a C-type pattern.

3 Molecular compositions of starch granules

3.1 Polysaccharide components

Normal starch, such as normal maize, rice, wheat and potato, contains about 70–80% amylopectin and 20–30% amylose. The methods commonly used to assess the apparent amylose content of starch rely on the iodine affinity of a defatted starch solution [19] and the blue colour derived for the amylose complex of iodine [20–22]. However, the results are affected by the presence of lipids and the structure of amylopectin, as the long chains of the latter component can also complex with iodine and increase the iodine affinity and resulting blue colour. Other methods have also been described, of which an enzymatic debranching and subsequent analysis of long (amylose) and short chains (amylopectin) was found most accurate [23]. The amylose content of waxy starches is small; being less than 1% in waxy maize starch and up to 8% in waxy barley. High amylose starch contains up to 80% apparent amylose. The amylose content of potato starch, having

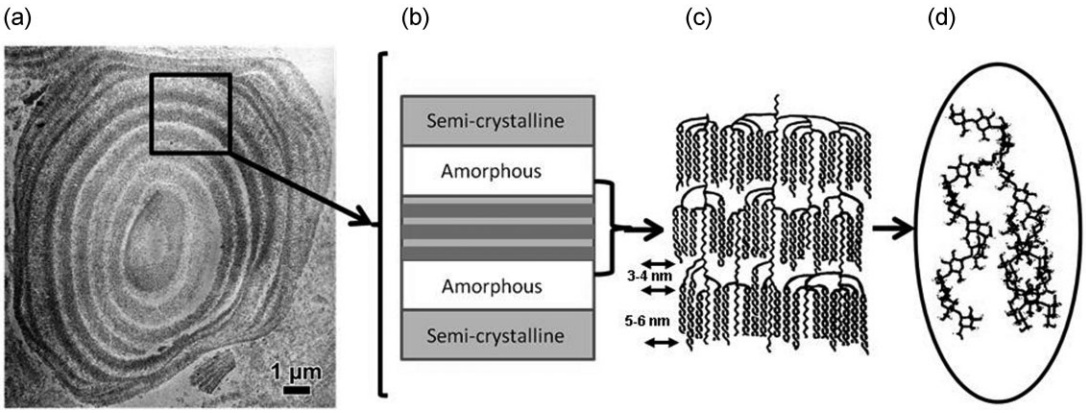

Figure 3. From growth rings to amylopectin. Schematic representation of the several level of ultrastructure of starch: (a) Ultrathin section of a waxy maize starch granule after 7 days of H_2SO_4 hydrolysis and staining with uranyl acetate and lead citrate (Courtesy of I. Paintrand, CERMAV); (b) alternation of semi-crystalline and amorphous rings; (c) clustered model of amylopectin; (d) branching a double-helix onto a single helix (adapted from ref. [248]).

different granular sizes and of starch at different radial locations varies from 17 to 21%.

Materials having structures and properties in between the linear amylose molecules and the large amylopecin molecules are found in starch granules. Such an intermediate material has been isolated and the structures studied extensively indicated a heterogeneous nature [24]. Some amylose molecules consisting of branches which displayed smaller iodine affinity have been described [25]. Amylose–iodine complexes display a deep blue colour, which is the result of an electron relay on the polyiodide ions [26] induced by an alignment of iodide in the groove of the helical structure.

Phytoglycogen, a water-soluble polysaccharide, is found in sugary-1 maize endosperms [27–29]. It has an average branch CL of degree of polymerization (DP) 10.3 which is shorter than that of waxy maize amylopectin that has a DP of 18.5 [29].

3.2 Minor components

Beside the major polysaccharide components, starch granules also contain very small amounts of proteins, lipids and phosphorus. The protein content is in the order of 0.1–0.7% by weight [30–33]. Granule-bound proteins were found at both the surface of granules and in interior parts. Some starch granules (*e.g*. maize, sorghum and wheat, but not rice, potato and tapioca) contain tiny pores or channels that extend from the granule surface into the interior parts [34, 35]. In sorghum, the diameters of the external openings of the pores are about 0.1–0.3 μm and that of the internal channels are about 0.07–0.1 μm. These pores and channels are not artefacts. At germination they apparently act as the target place for amylolytic enzymes that enlarge the pores into tunnels, from where they can digest the granule [36]. There exits a direct correlation between the frequency and distribution of these pores, and the enzymatic digestibility of the starch granule.

Han *et al*. [37] showed that the channels are filled with proteins, of which a major protein was identified as brittle-1 (a protein associated with the *brittle-1* mutation in maize). In normal potato, maize and wheat starch granules, but not in amylose-free potato and waxy maize, granule-bound starch synthase (GBSS, a protein responsible for amylose synthesis) was located to internal concentric spheres and the central cavity. These special places were, therefore, suggested as the location of amylose synthesis [38].

Lipids are also found in low amounts (up to 1.5%) in many starches, especially cereal starches, in the form of free fatty acids and lysophospholipids [39]. Some starches, *e.g*. from potato and many legumes, have very low lipid content or are practically lipid free [22, 30]. The lipids in cereals are associated with the amylose fraction [39]. In these plants, the proportion of lipid-complexed amylose varies from 13 to 43%, the rest of the amylose is lipid free. In low amylose (waxy) barley and maize the lipid-complexed fraction was reported to amount 19–62% [40, 41].

Almost all starches contain phosphorous of certain forms [42], which is found in the phospholipids and as phosphate monoesters. Starch phospholipids and phosphate monoesters have different effects on starch paste properties. Phospholipids, as those found in cereal normal starches, decrease the paste clarity [43]. Phosphate monoesters, mainly found in potato and other starches increase the paste clarity and paste viscosity [44, 45]. Starch phosphate monoesters in native starch are essentially found in amylopectin. Potato starch has unusually high phosphate monoester content. This amounts to one phosphate monoester per 317 glucose units [46], which is

equivalent to one phosphate in 13 branch chains. Some are present in the crystalline region of potato starch and are protected from acid hydrolysis.

4 Structures of amylose

4.1 Chemical structures of amylose

Starches in general possess a rather broad molecular weight distribution of its amylose fraction with weight-average values much higher than number-average. The size of the polymers, more frequently given as the DP than molecular weight values, differs both between and within plant species. Thus, amylose from barley [47] was reported to have DP_n 1570 (DP_w 5580) and maize [48] possessed DP_n 930–990 (DP_w 2270–2500). The DP_n in different wheat varieties ranged from 830 to 1570 [49]. The size distribution, obtained by SEC, within a tapioca sample ranged from DP_w 580 to 22,400, whereas in kuzu the distribution was narrower, in the order 480–12,300 [50].

Most starches contain a mixture of linear and branched amyloses [6, 51]. The molar fraction of branched amylose varies between samples from 0.1 to 0.7 and the molecular weight is generally higher than for the linear amylose component [52]. The average number of chains in a single, branched molecule varies from 5 (rice and maize) to 21 chains (wheat) [49]. Wheat amyloses contain, in addition to chains with several hundreds to thousands of residues, also small amounts (3.2–7.6% weight basis) of very short chains [49]. This was also the case in a fraction isolated from maize amylose and [53] suggested that the short chains comprised small clusters along the long chains. It was also shown that amylose of high molecular weight in maize and rice contains a higher proportion of the very short chains than smaller amylose molecules [54]. The actual unit chain distribution in branched amyloses is not known, because the components cannot be separated from the linear portion. However, the exoacting enzyme β-amylase hydrolyses every second α-(1–4)-linkage from the non-reducing end of the polysaccharide chains until it reaches a branch point that block a further degradation. The linear amylose is thereby completely hydrolysed into maltose (and small amounts of maltotriose), whereas all the branched amylose is reduced into β-limit dextrins (β-LD) that contain all branches and the residual, internal chain segments. DP_n of the β-LD of amyloses from different sources range from 700 to 2000 and the average chain length (CL_n) from 50 to 160 [52, 55].

4.2 Single helical structures of amylose

In a freshly prepared aqueous solution, the amylose chain adopts a random coil structure [56], which is, however, not stable. Amylose tends to form, in an instant reaction, single helical inclusion complexes with suitable complexing agents [57]. The single helical (inclusion) complex was first reported by Katz and van Itallie [58]. After cooking, dough develops an X-ray diffraction pattern, which differs from the original A, B or C patterns [59] that was named V-pattern from the German word 'Verkleisterter starke' meaning gelatinization (Fig. 4).

Single amylose chains have a unique ability to form complexes with a variety of complexing agents. Monoacyl lipids and emulsifiers as well as smaller ligands, such as alcohols or flavour compounds are able to induce the formation of left-handed amylose single helices, displaying the V-type diffraction pattern. Depending on the size of these complexing agents, the amylose chain can take up a helical structure having either six, seven or eight glucose units per turn; helical structure with seven glucose units per turn are under discussion in the literature. The structure of these amylose helices has a lamellar thickness of about 10 nm [60–63]. More relevant to the structural understanding of the molecular components of starch, are the amylose–lipid and amylose–fatty acid complexes. Differential scanning calorimetry studies of normal cereal starches, such as maize and wheat, show an additional thermal transition peak at higher temperature than the starch gelatinization peak (Fig. 5) [64–66].

This peak disappears after the lipid is removed from the starch; it reappears after the addition of lipids [67]. It is therefore attributed to the melting of the amylose–lipid complex. In the native starch granule, the starch–lipid complex is in an amorphous state. It can be annealed into a more ordered semi-crystalline form, presumably in a lamellar form, which displays a V-type X-ray diffraction pattern. Except for high-amylose maize starch [68], the V-type pattern is rarely seen. From studies using ^{13}C-cross polarization/magic angle spinning, [69] the occurrence of amylose–lipid complexes has been quantified. The results

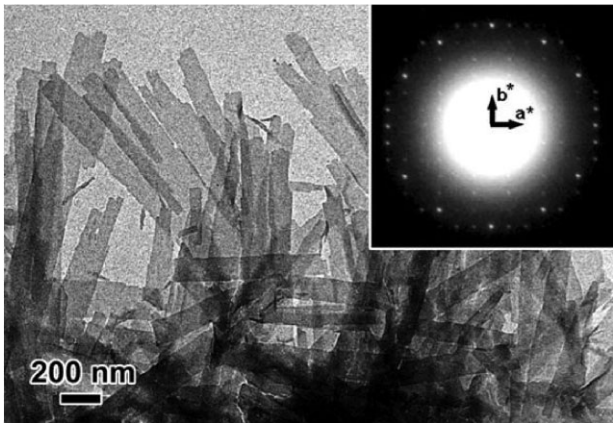

Figure 4. Electron diffraction pattern recorded from of *in vitro* grown V type amylose (micrographs).

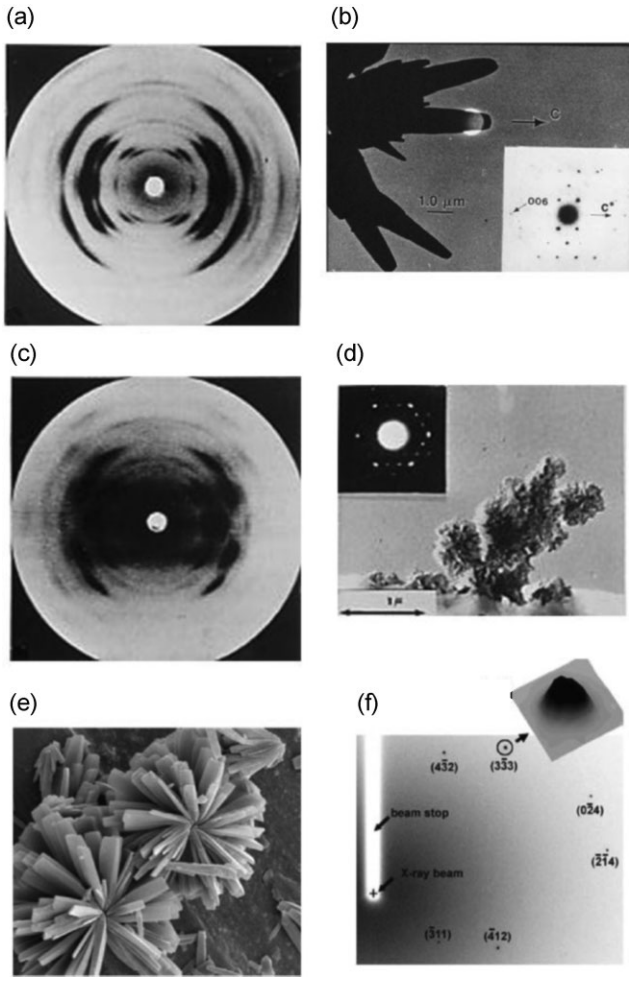

Figure 5. (a) X-ray fibre diffractogram recorded for A-type starch; (b) microcrystal of A-type starch observed by low dose electron microscopy (inset: the electron diffraction diagram recorded under frozen wet conditions) taken from ref. [249]; (c) X-ray fibre diffractogram recorded for B-type starch; (d) microcrystal of B-type starch grown as spherulites observed by low dose microscopy (inset: the electron diffraction diagram recorded under frozen wet conditions) taken from ref. [90]; (e) scanning electron image of A-type starch prepared by recrystallization of synthetic amylose; (f) one quadrant of a typical X-ray diffraction diagram of a crystal, as in (e) obtained in 1 s during 2° rotation, using 10 mm collimated beam at the ID13 beamline of the European Synchrotron Radiation Facility (Grenoble, France) (taken from ref. [93]).

showed that up to 43% of amylose in non-waxy rice starch, 33% in oat starch, and 22% in normal maize and wheat starch granules, are complexed with lipids with a single helical conformation. The remaining amylose is free of lipids and occurs in a disordered conformation. Phospholipids, monoglycerides and fatty acids are good complexing agents and can participate in the formation of complexes with single amylose chains (Fig. 6).

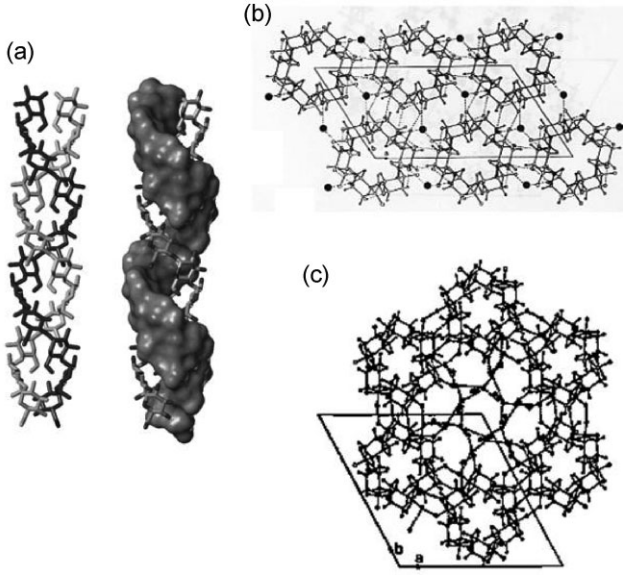

Figure 6. 3D structures of A-type and B-type crystalline polymorphs. (a) The double helices are left handed and parallel stranded. (b) Structure of A starch. Chains are crystallized in a monoclinic lattice. In such a unit cell 12 glucopyranose units are located in two left-handed, parallel-stranded double helices, packed in a parallel fashion. For each unit cell, four water molecules (closed circles) are located between the helices. Projection of the structure onto the (a, b) plane. Hydrogen bonds are indicated as broken lines [89]. (c) Structure of B starch. Chains are crystallized in a hexagonal lattice, where they pack as an array of left-handed parallel-stranded double helices in a parallel fashion. Thirty six water molecules represent 27% of hydration. Half of the water molecules are tightly bound to the double helices, and the remainder form a complex network centred around the sixfold screw axis of the unit cell. Projection of the structure onto the (a and b) plane. Hydrogen bonds are indicated as broken lines [90].

The characteristic V-type 3D structures obtained with linear alcohols and fatty acids have been extensively investigated. The typical chain conformation is in a helical left-handed conformation with six residues per turn; the pitch height varies between 7.92 and 8.04 Å. In the presently accepted model for amylose–lipid complexes, the aliphatic part of the lipid is included inside the amylose helix, whereas the polar group is lying outside, being too large to be incorporated [70].

4.3 Double helical structure of amylose

In the absence of complexing agents, amylose molecules gradually associate with a rate that depends on the molecular size [71–78]. A minimum CL of DP 10 is required for double helix formation in a pure oligosaccharide solution [79–81]. Shorter oligosaccharides such as maltohexaose

can co-crystallize in the presence of longer chains [79]. These results indicate that DP 6 is the shortest branch CL found in amylopectins of all native starches.

Structures of retrograded double helical amylose have been investigated by X-ray fibre diffraction methods [82–84] using methodology summarized in ref. 85. They display A- and B-type X-ray diffraction pattern [59, 86, 87]. Similar observations were made for the single crystals grown *in vitro* [88] from monodisperse fractions of amylose having DP 15 and DP 30, which give rise to a powder diffraction pattern typical of the A- and B-type, respectively.

The 3D structures of the crystalline arrangements corresponding to the A- and the B-type have been elucidated throughout the joint use of X-ray fibre diffraction, electron diffraction and molecular modelling [89, 90] and crystallographic study of small oligosaccharides [91, 92]. The crystal structure of A-type starch has been revisited using synchrotron radiation (SR) microdiffraction data collected from individual micron-sized single crystals analysis of single crystal. Whereas all the main features of the original structure determination are corroborated, this new investigation provides the unambiguous location of a new water molecule bringing as 1.622 the calculated density of the A-type crystal [93].

The double helices in both A- and B-type are left handed and parallel stranded. They are almost perfectly sixfold structure, with a crystallographically repeating unit of 10.5 Å. The symmetry of the double helices differs slightly in A- and B-structure. In the A-form, the repeated unit is a maltotriosyl unit, whereas a maltosyl unit makes up for the repeat of the B-type. Independent evidence about the nature of these repeated units have been gained from solid-state ^{13}C-NMR, as the C-1 peak in the A-form is a triplet, whereas it is a doublet in the spectrum of the B-form [94]. In the A- and B-allomorphs, the observed space group imposes the parallel arrangement of all double helices. The double helices of both forms are packed in hexagonal or pseudohexagonal arrays. The void in the lattice of B-starch, which accommodates numerous water molecules, is not present in A-starch. In both arrangements, there is a pairing of double helices that corresponds to 1.1 times the distance between the axes of the two double helices. A relative translational shift of 0.5 nm along the orientation of the chains allows a very close nesting of the 'crests' and 'troughs' of the paired double helices. Such a dense association, which is strengthened by O-2..O-6 and O-4..O-3 hydrogen bonding, corresponds to the most energetically favoured interactions between two double helices, as shown by theoretical calculations [95]. Therefore, the observed crystal structure of both polymorph A and B of crystalline starch can be rationalized, based on energy calculations, and key structural components have been identified. Among all possible arrangements, only two appear to be sterically favoured. These two types of arrangements of double helices are found in the A-polymorph. The B-polymorph is based on only one type that is favoured by the duplex of parallel double helices. These calculations could rule out the possibility of forming another stable 3D arrangement, and consequently the occurrence of the C-polymorph.

The conditions required to generating either the A- or B-starch crystal conformation are reasonably well understood. Under cool, wet conditions (such as in a potato tuber) B-starch crystals form, while in warmer, drier conditions (*e.g.* in a cereal grain) the A-allomorph is preferred. Amylosic CL also affects the selection of crystal form, amylose fragments with a DP$<$10 do not crystallize; chains with a DP from 10 to 12 tend to form A-starch, whilst chains with a DP$>$12 tend to yield the B-form. This is likely to result from the difference in the loss of entropy upon crystallization experienced by chains of different lengths. The allomorphic transition in native starch and amylose spherocrystals monitored by *in situ* synchrotron X-ray diffraction [96].

5 Structures of amylopectin

5.1 Chemical structure of amylopectin

The molecular structure of the major, extensively branched starch component is considerably more complex than that of amylose. Generally, the amylopectin is also considered as a much larger macromolecule than amylose. Reported M_w values are 2–700 $\times$ 10^6 [97–101]. Numeric values are considerably lower, however. The reducing end residue was labelled with a fluorescent dye and analysis of the size distribution showed that several amylopectin samples were mixtures of three molecular species [102]. The DP_n values ranged from 0.7 to 26.5 $\times$ 10^3, which is only slightly higher than corresponding values for amyloses. In this section, we discuss the primary and secondary structures that describe the composition of unit chains and the organization of these chains into clusters. The tertiary and quaternary structures that describe the conformation of the chains in helical order and the organization of amylopectin into starch granules together with amylose is discussed in a later section.

5.2 Unit chain distribution of amylopectin

To be able to distinguish and describe the unit chain composition of amylopectin (and similar branched polysaccharides), the chains are grouped into certain categories. Somewhat different divisions of the chains have been described and depend mostly on the method applied for their analysis. Peat *et al.* [103] made a basic division of the chains in 1952. They defined A-chains as

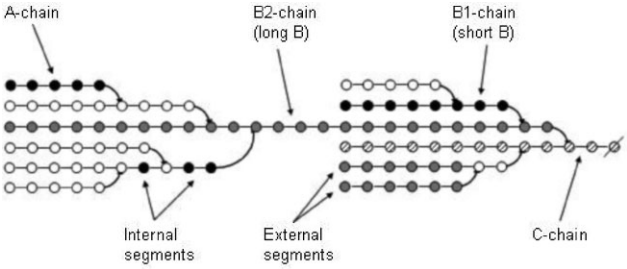

Figure 7. Basic labelling of chains in amylopectin. Circles denotes glucosyl residues, horisontal lines (1–4) and bent arrows (1–6) linkages. The reducing-end residue is to the right.

being unsubstituted by other chains and connected through a (1–6)-linkage to the rest of the macromolecule. In contrast, B-chains are substituted by one or several other chains (A- and/or B-chains). In addition, each macromolecule contains a single C-chain, which carries the sole reducing end group (Fig. 7). Hanashiro *et al.* [104] described the distribution of C-chains after labelling with a fluorescent dye. The chains covered the DP range 10–130, possessing a peak in size-exclusion chromatograms at DP 40 for several amylopectin samples.

Analysis of the size distribution of the unit chains of amylopectin became possible for a broader community with the commercialization of the enzymes isoamylase and pullulanase that specifically attack α-D-(1–6)-linkages in amylopectin and similar polymers. The debranched sample is analysed by gel-permeation chromatography (GPC) or high-performance SEC (HPSEC). Very high resolution up to DP around 60 is obtained by high-performance anion exchange chromatography (HPAEC) or by capillary electrophoresis. A typical unit chain distribution profile is shown in Fig. 8.

The average CL of most amylopectins is 17–26 and depends on the type of crystallinity of the granular starch. A-crystalline starches possess typically shorter CL than B-crystalline types [105]. However, the average CL value gives only a poor description of the true structure of amylopectin, because all samples (from normal types of starch) possess in fact two major groups of chains, short and long. The molar ratio of short to long chains differs between starches from different sources from approximately 4–19. B-crystalline samples have typically lower ratio than A-crystalline types [104, 106].

Hizukuri [107], working with HPSEC, found that the chains of amylopectin possessed a characteristic periodicity in length (approximately CL 25–30) and subdivided the long chains (presumably representing B-chains) into B2- (CL ∼45), B3-chains (CL ∼70), *etc*. The major group of short chains, with its characteristic peak around DP 11–15, was suggested to build up clusters of chains and was a mixture of short B-chains (B1-chains) and A-chains. Later,

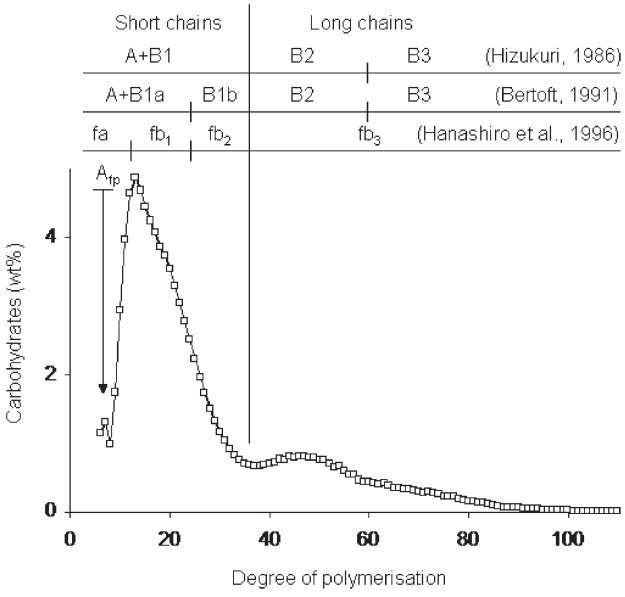

Figure 8. Unit chain distribution obtained by HPAEC of debranched sweet potato amylopectin. Values at DP >60 are approximative. Divisions of chains into categories presently mostly used as suggested by different authors are indicated. A_{fp} denotes 'fingerprint A-chains', a subgroup of A-chains at DP 6–8 [120].

[108] compared unit chain profiles obtained by HPAEC from a lot of different starches and described a shorter periodicity in length (CL ∼12). The shortest group (named fa) had CL from 6 to 12 and was suggested to represent the A-chains. However, it is now known that fraction fa only represents a part of the A-chains [106]. The amount of this group correlated with the crystallinity type and the average CL of the whole amylopectin sample, so that high amounts were found in A-crystalline samples that possess short CL, and *vice versa.* The group named fb_1 at CL 13–24 was B1-chains and group fb_2 (CL 25–36) was presumably B2-chains. (Thus, unfortunately, the originally defined B1-chains were redefined as B1 and B2.) Finally, chains at CL>37 (group fb_3) were not resolved into subgroups (Fig. 8). It is of special interest to notice that the division of chain fractions according to Hanashiro *et al.* [108] in several reports was shown to correlate with the gelatinization of the crystalline structure inside the starch granules [109–115]. Thus, fraction fa correlates negatively with the melting temperature of the crystals, whereas fb_1 correlates positively. It was suggested that the short chains, which do not readily form double helices, introduce structural defects into the crystalline lamellae of the granules and thereby interfere with the organization of the crystals [109–114, 116, 117]. Bertoft [118] isolated groups of chains from maize amylopectin of intermediate lengths between the long chains and the major group of short chains. These were considered as subgroups of

the originally defined B1-group and named B1b and B1c (corresponding to fb_2), whereas the shorter, major group was B1a.

It is interesting to notice that the shortest CL found in any amylopectin sample is six [119]. Further, the distribution of the short chains at CL 6–17 is very characteristic for amylopectins from different samples and was characterized as a 'fingerprint' of the sample [119]. Chains at CL 6–8 that constitute a subgroup of A-chains were named 'fingerprint A-chains' and designated A_{fp} [106, 120].

In addition to the groups of chains at CL up to ~100, the literature contains also reports on 'extra long' or 'super-long' chains with CL of the same order as amylose type of chains [121]. Such chains were found in maize [48], wheat [49], barley [47], rice [110, 122], potato [123], and cassava [124]. On a molar scale, the number of these chains is very low, perhaps one or a few per macromolecule. On a weight basis, the amount is around 1–10%. Several rice starch samples, notably those of *indica* varieties, were reported to contain as much as 14–20 wt% of 'super-long' chains [125]. As a result, when the amylose content is estimated from iodine affinity values [125] or as the amount of very long chains in the debranched starch samples [110], the apparent amylose values are strongly overestimated. The enzyme GBSS (normally involved in amylose synthesis) is responsible for the synthesis of the 'super-long' chains in amylopectin [126, 127].

5.3 The internal structure

Though the unit chain distribution of amylopectin gives an overview of the composition of chains, it does not describe the organization of these chains. A complementary picture of the internal amylopectin structure is needed and is obtained from the unit chain profile of limit dextrins. As described above for amylose, the enzyme β-amylase removes the external chains from amylopectin. The β-amylolysis limit is typically 52–58% [128]. The resistant β-LD contains very short A-chain stubs in the form of maltosyl or maltotriosyl residues, whereas the external length of the B-chains is reduced into only one or two residues (depending on if the chain originally had an odd or even number of residues) [129]. The enzyme phosphorylase a from rabbit liver also removes the external chains (by phosphorolysis resulting in glucose 1-phosphate production). In the ϕ-LD all A-chains correspond to maltotetraosyl units [130] and external B-chains to maltotriosyl stubs [131, 132]. If the ϕ-LD is treated with β-amylase, each external chain stub in the resulting ϕ,β-LD is further reduced by a maltosyl residue [131]. Thus, regardless the original length, all A-chains in the ϕ- or ϕ,β-LD are reduced into 4 or 2 residues, respectively, and all B-chains are longer. After debranching and chromatographic analysis of the composition of unit chains, the ratio of A/B-chains is obtained [132]. In most samples the ratio is 0.8–1.5 [106, 128].

The internal unit chain distribution of the ϕ,β-LD was analysed in several amylopectin samples [106]. The same major groups of chains as found in the original amylopectins (short chains and the long B2- and B3-chains), are generally clearly distinguished in the ϕ,β-LDs. This suggests that the distribution of groups of chains according to their length stems from the internal structure of the macromolecule and that the length of the external segments are fairly uniform, possibly close to the average value (varies from 11 to 17, depending on sample and laboratory report). On the basis of the shape of the chromatograms, the short B-chains (BS) of the LDs were subdivided into a major group, BS_{major}, at CL 8–25, and a minor group at CL 3–7 that seemed characteristic for a certain LD-sample and was therefore named 'fingerprint B-chains', B_{fp}, in analogy to A_{fp} [106, 132]. Yao *et al.* [133] made a similar subdivision into B1a- and B1b-chains, which corresponds to B_{fp} and BS_{major}, respectively (Fig. 9).

On the basis of the internal size distributions, the amylopectin samples were divided into four characteristic groups [106] (Fig. 9). Group 1, consisting of barley, rye and oat starches, as well as amylopectin from the root of Andean yam bean, which all possessed A-crystalline granules, was characterized by a low content of long chains and a broad size-distribution of the short B-chains leading to

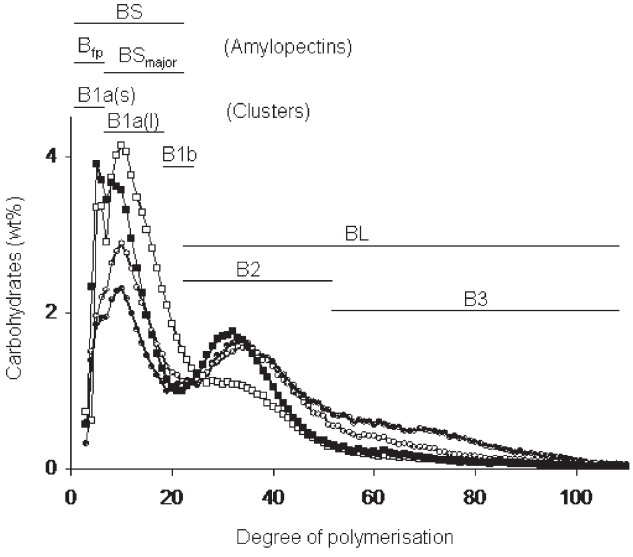

Figure 9. Internal B-chain profiles of amylopectins obtained by HPAEC of debranched ϕ,β-LD from group 1 (□, represented by oat), 2 (■, rice). 3 (○, arrowroot) and 4 (●, yam). Chains were divided into different categories as shown. The subdivision of short (BS) chains in amylopectins is based on the two major groups B_{fp} and BS_{major} [106], whereas a different subdivisions are more useful for clusters isolated after α-amylase treatment.

poor separation of these major chain categories in the chromatograms. Group 2, which included both A-crystalline (maize and rice) and C-crystalline (kudzu and sago) starches, contained considerably more B2-chains and possessed a narrower size-distribution of the short chains.

In both groups the B_{fp}-chains were generally clearly distinguished as a separate category (with the exception of Andean yam bean). The third group also consisted of A- (cassava and mung bean) and C-crystalline (arrowrooth) starches. When compared to group 2, the samples of group 3 were characterized by a somewhat higher content of long B-chains and the B_{fp}-chains were only distinguished as a more or less weak shoulder in front of the BS_{major}-chains in the chromatograms. A similar profile of the short chains was possessed by group 4, which hosted all B-crystalline samples (potato, edible canna and lesser yam). This group was distinguished from group 3 mainly by a high content of the long B3-chains.

5.4 The cluster structure

The model of the cluster structure of amylopectin was introduced around 1970 [134, 135], primarily based on structural studies of acid-treated starch granules [136]. Such treatment results in a highly crystalline product containing mostly short chains from amylopectin [137–139]. A major part of the branches are removed by the acid, suggesting that they are found in groups, as clusters, in the amorphous parts of the granules [140–142]. Though only few, minor modifications were made to the basic concept [107, 136, 143, 144] and the model is generally accepted, rather little is truly known about the structure of the clusters and most discussions are based on indirect evidences. Until recently, a basic definition of a cluster was still missing, and this is probably – at least partly – a reason for the great diversity in the suggested size of clusters found in the literature ranging from an average of 4.22 chains up to 34 chains [11, 145]. It was estimated that a single, large amylopectin macromolecule with DP_n in the order of $10–16 \times 10^3$ is build from 60 to 120 U of clusters [102].

Rather few attempts have been made to study clusters in isolated form. According to the accepted model [107], the long B-chains are involved in the interconnection of the clusters of short chains. Endoacting amylolytic enzymes were therefore used to cleave the intercluster segments (IC-S). Bender *et al.* [146] used cyclodextrin transferase (CGT) to isolate branched, intermediate products suggested to represent clusters from waxy maize and potato amylopectin. In both samples they found three major size groups of clusters that as β-LDs had DP from 40 to 140 (and thus the original clusters including the external chains were of roughly double size). Finch and Sebesta [147] used a maltotetraose-forming enzyme from *P. stutzeri* and found that both potato and wheat amylopectins contained clusters of uniform size, but the clusters in potato were approximately three times larger (DP ∼140 as β-LD). Bertoft and co-workers have used the α-amylase of *B. amyloliquefaciens* (also called the liquefying enzyme of *B. subtilis*) and GPC to study the pattern of cluster sizes in several amylopectins. In their work, the criteria for a cluster is a drastically reduced rate of hydrolysis compared to the initial stages of amylopectin degradation [148] and, from structural analyses of the intermediate dextrin products, a cluster was defined as a group of chains, in which the branches are separated by internal chain segments shorter than nine glucosyl residues [149]. Generally, A-crystalline samples tend to have larger clusters than B-crystalline samples. The size distribution of limit dextrins of the clusters in maize, barley and rice was comparatively broad with peak-DP (representing the major part of the clusters on a weight basis) in GPC around 100–200 [23, 143, 150–152]. Other A-crystalline samples possessed narrower size distributions; in cassava peak-DP was 104–129 and in amaranth around 82 [153, 154]. In the B-crystalline samples *amylose-extender* waxy maize and potato DP was 50–75 [23, 155, 156]. Small clusters (generally only representing a minor group of clusters) had similar DP (25–35) in all samples. The number of chains that comprise a large cluster was estimated to 23 in waxy rice amylopectin. Small clusters were composed of 5–8 chains [157]. The density of branches within clusters of the A-crystalline samples from cereals was higher than in the B-crystalline samples analysed so far [23, 153, 157], but in the A-crystalline root starch of cassava the density was similar or only slightly higher [154].

The unit chain composition of isolated clusters from maize, rice, amaranth, cassava and potato was also analysed [143, 153–157]. In all cases the long B-chains were cleaved by the α-amylase, clearly showing that they are involved in the interconnection of the clusters. In many cases, however, small amounts of long chains still remained in fractions characterized as clusters on the basis of a very slow hydrolysis rate. It is interesting to notice that chains of intermediate lengths, largely corresponding to the minor group of B1b-chains already existing in amylopectin (in LDs approximately DP 18–24), were preferentially formed in all samples as a result of the enzymatic attack. This suggests a common mode of cluster structure and interconnection. Smaller chains (B1a) were also apparently formed from cassava and potato amylopectins, but in rice amylopectin such chains were found in increased amounts only in very small clusters. In ϕ,β-LDs of clusters from the latter amylopectin, however, high amounts of chains at DP 3 were detected. A similar result was found in clusters of amaranth and suggests that at least in these samples the intercluster chain has a

specific structure with a very short internal chain at the reducing-end side [153, 157].

5.5 The building block structure of clusters

The branches are apparently not evenly distributed within the clusters, but found in small groups. These groups were called building blocks and were isolated from clusters by an extensive hydrolysis with the *B. amyloliquefaciens* α-amylase [23, 149, 152, 153]. The DP of building blocks varies largely from 5 to 40 and were grouped into types 2–7 with a corresponding estimated number of chains from 2 to 7. The size distribution was comparatively broad in the large clusters of waxy rice and *waxy-dull* maize [23, 152]. In potato and amaranth, the blocks were smaller and type 2 – with only two chains – preponderated [149, 153]. The average DP of the building blocks in amaranth and potato (10.7–12.7) was therefore smaller than in rice and *waxy-dull* maize (12.7–17.1), whereas the density of blocks in the clusters tended to be slightly higher. The number of building blocks that build up a cluster varies with the size of the blocks and the clusters.

As so far only very few samples have been analysed in more detail, it is not possible to give a generalized description of the building block structure of clusters. Nevertheless, it was found that the branching density (or degree of branching, DB) within the building blocks is high: in amaranth ∼14% and in potato 16–17% [149, 153]. The internal chain length (ICL) is therefore short: 2.8 and ∼2.0 in amaranth and potato, respectively. In comparison, the ICL of the clusters in the two amylopectins is ∼4.4 and 4.3–6.4 and shows that the interblock chain length (IB-CL) is rather long. In fact, IB-CL was estimated to be 6.8 in amaranth, whereas in potato it ranged from 7.1 to 8.5.

Based on the composition of building blocks, the clusters from waxy rice amylopectin were structurally divided into two distinct groups [152]. It was suggested that these groups originated from structurally different domains. Whether such domains are found on an intra- or intermolecular level, or possibly intergranular level, is not known. Also in potato it was found that domains with structurally slightly different clusters existed. One type possessed building blocks with average DP of 10.9. The density of blocks was 7.2 and the IB-CL was 7.1. In another type the values were 12.7, 5.8 and 8.5, respectively [149].

5.6 The organization of categories of chains in amylopectin

In its native configuration in starch granules, amylopectin participates in both crystalline and amorphous structures that are further discussed in detail in the next section of this review. The external chains form double helices that crystallize into a thin lamella, behind which an amorphous lamella is found, together forming a 9 nm repeat distance that build up semi-crystalline rings [158]. The major part of the branches in amylopectin is found within the amorphous lamellae. The internal chain segments between branches are therefore amorphous. The average chain length of the internal segments (ICL) in amylopectins is 4–9 residues, depending on starch type and report [106, 128]. Basically, three types of internal segments exist, namely between clusters, between building blocks inside clusters and inside building blocks. The actual size distribution of these segments cannot be experimentally analysed, but indirectly it is possible to estimate their average lengths and thereby obtain a better understanding of the structural role of the different chain categories.

As the average ICL of building blocks is only 2–3, the branches in these densly packed areas are problably separated by some 1–4 glycosyl residues. Analyses of the chain distribution in the building blocks of potato clusters showed two size groups at DP 2 and 3–8. The former represented short A-chain stubs that either were originally already found in the amylopectin macromolecule or were formed as a result of α-amylase attack at the interblock chain segments [149]. Some of the chains with DP 3 were possibly also A-chain stubs, but the rest of the latter chains were short B-chains. Again, some of them were formed during α-amylolysis, but others corresponded to the 'fingerprint B-chains' (B_{fp}) of the amylopectin (Fig. 9). Thus, B_{fp}-chains participate typically in building blocks with three or more chains, in which the B_{fp}-chain is attached to another chain and carries one or two chains in proximity to its reducing end side (Fig. 10) [155, 159].

Figure 10 shows a model of the building block structure of the ϕ,β-LD of a cluster from amaranth starch based on the structural data given by Kong *et al*. [153]. The cluster with a DP of 82 consists of six building blocks, one longer

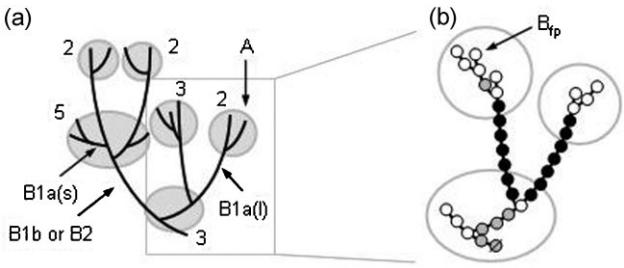

Figure 10. A model of the building block structure of a cluster in amaranth amylopectin as a ϕ,β-LD based on data given by Kong *et al*. [153]. (a) Building blocks are encircled and numbered according to their number of chains. Different categories of chains are indicated. (b) An enlargement of a part of the cluster. Circles symbolize glucosyl residues, of which black are residues in the IB-S and grey are internal residues of the blocks.

B1b- or B2-chain (that was formed by the α-amylase when the cluster was isolated), and the rest are B1a- and A-chains. Longer B1a-chains (B1a(l)) possess DP at 8∼17 in the ϕ,β-LDs of amylopectins (Fig. 9).

Approximately, three such chains were found in the amaranth cluster. As the interblock CL is ∼7, their length strongly suggests that they are involved in the interconection of two building blocks inside the cluster [149]. The length of the B1b-chain is 18–22, which suggests that it spans over three building blocks. As some clusters possessed even longer chains with DP up to ∼45 (corresponding to B2-chains) they might be involved in the interconnection of up to five blocks. It is thus highly interesting to notice that the structure in Fig. 10 suggests a periodicity of roughly 10–12 residues in the chains that interconnect the building blocks, which coincides with the periodicity found by Hanashiro *et al.* [108]. Thus, rather than reflecting the interconnection of clusters, as it was suggested, it seems that the periodicity stems from the interconnection of building blocks.

In the cluster structure proposed by Hizukuri [107], a cluster is build from A-chains (that are the shortest chains) and B1-chains. The clusters are interconnected through the long chains, so that B2-chains are involved in the interlinkage of two clusters and B3-chains of three clusters, *etc*., thus matching a periodicity in CL of approximately ∼25 and the alternating lamellar structure inside starch granules (Fig. 11a). In the model, the long B-chains are integrated parts of the clusters with some segments participating in crystalline areas and some segments being amorphous. As shown by O'Sullivan and Pérez [161], however, amorphous chain segments can be found in several directions and the ICL of the long B-chains is therefore not necessarily correlating with the thickness of the amorphous lamella.

Bertoft [132] discussed alternative modes of cluster interconnections that cannot be distinguished from the model of Hizukuri on the basis of the unit chain profile of amylopectin. One was a two-directional backbone model, in which the direction of the clustered chains is (more or less) perpendicular to the direction of the backbone (Fig. 11b). This has a dramatic effect on the direction of the crystalline and amorphous lamellae. As discussed above, acid-treated starch granules lack long chains. In the two-directional alternative the entire long B-chains are amorphous and are therefore removed by the acid completely [120, 132]. It was also noted that the 'fingerprint A-chains' at DP 6-8 are removed by acid and they were therefore also suggested to be amorphous [120]. These chains might therefore preferentially be found associated with the long B-chains in the backbone. In a slightly modified backbone structure suggested for potato amylopectin [149] some long B2-chains participate in both the clusters and in the amorphous backbone,

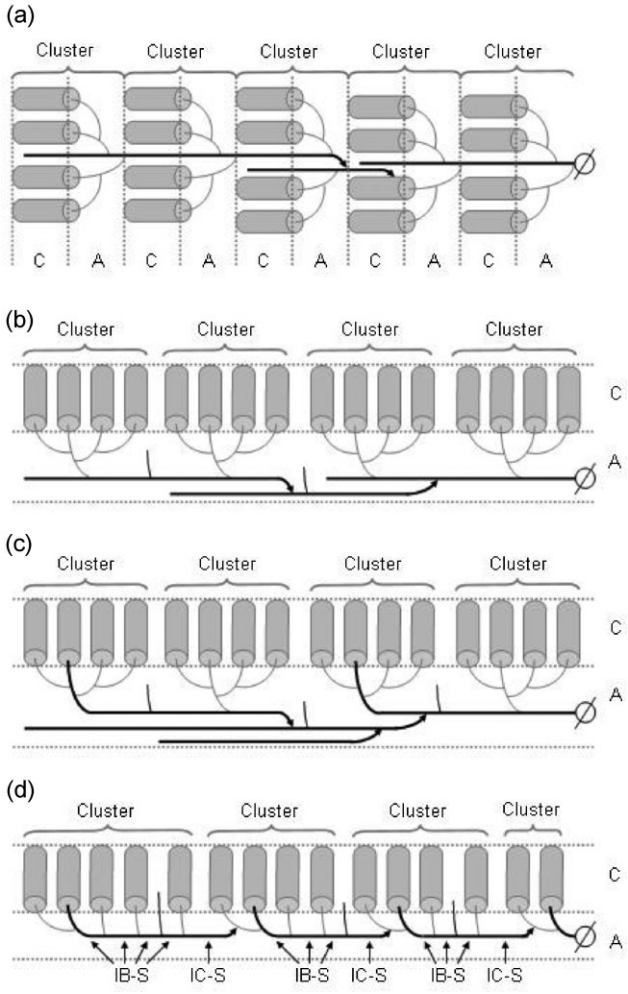

Figure 11. Alternative models of the organisation of clusters in amylopectin. Long chains (black, bold lines), short chains (grey, thin lines), the reducing end (⌀), and the amorphous (A) and crystalline (C) lamellae inside starch granules are indicated. External segments form double helices symbolized by grey cylinders. (a) The cluster model by Hizukuri [107], in which the long chains form an integrated part of the clusters. (b) A two-directional backbone model, in which the clusters are anchored in perpendicular direction to a backbone of completely amorphous long chains. Some A_{fp}-chains (black, thin lines) are associated with the backbone rather than the clusters [132]. (c) A backbone model, in which some B2-chains participate in the crystalline lamella through their external segment. Additional long chains can be found in the amorphous backbone [155]. (d) An alternative model, in which the clusters are integrated parts of the backbone through their IB-S. Clusters are separated by somewhat longer IC-S. A_{fp}-chains can introduce defects in the crystalline lamella [154].

whereas others (together with B3-chains) are only found in the backbone (Fig. 11c). This model is compatible with the experimental results showing that two clusters generally were interconnected by a single B2-chain, but when several clusters were isolated as a group (a structural domain) more long chains than predicted in the model by Hizukuri were involved.

Still another modification of the backbone model is shown in Fig. 11d. In this, the cluster itself forms a part of the backbone through its interblock segments (IB-S), rather than being attached to the backbone as a separate entirety [154]. Instead, the building blocks are directly attached to the backbone, and depending on the number of IB-S the length of the backbone chains varies considerably, which explains the existence of long B2-chains in some isolated clusters. This structure is also compatible with the liquid crystalline model of amylopectin suggested by Waigh *et al*. [162], where the building blocks would correspond to mesogens attached to the backbone through a flexible spacer arm.

If the chains connected to the backbone are very short, or not provided with a suitable flexible arm, they may introduce structural defects in the crystalline lamella rather that promoting crystallites [163–165]. In amaranth and cassava [153, 154] it was found that the clusters were separated from each other with intercluster-chain lengths (IC-CL) of 10–14 residues, *i.e*. only somewhat longer than the IB-S. Thus, the principle difference between blocks and clusters might be a question of a few glucosyl residues, as only a small elongation of an IB-S will result in an IC-S instead (Fig. 11d).

5.6.1 Phosphate monoesters

An enzyme, glucan water dikinase (GWD), was found to be responsible for the phosphorylation of amylopectin in potato [166, 167]. The protein structure and the properties of the enzyme were characterized [168, 169]. The phosphate is donated from adenosine triphosphate (ATP) to the C-6 position in the glucosyl residues [167]. Recently, another enzyme called GWD3 [170] (or phosphoglucan water dikinase (PWD) [171, 172]) was found to further phosphorylate the product of GWD at the C-3 position. As a result about 70% of the phosphate in amylopectin is at the C-6 position and the rest at C-3 [7, 173]. Longer chains act as better substrates for GWD [167, 168], and the degree of phosphorylation is correlated to the CL of amylopectin [173]. On a molar basis approximately 50% of the phosphorylated chains belong to the category of long B-chains (CL$>$35) and the rest are B1-chains, whereas A-chains apparently are non-phosphorylated [123]. Though GWD was reported to have a recognition requirement for the α-(1–6)-linkage [168], the phosphate is not found at the direct vicinity of the branch points, neither is it found closer than nine glycosyl residues from the non-reducing end of a chain [46]. The latter finding is interesting as it suggests that the external CL of the B-chains is at least nine residues.

Within potato starch granules phosphate is more associated with the interior parts (hilum) than peripheral parts. Jane and Shen [174] showed that this correlated with the fact that the B2- and B3-chains of the amylopectin are longer than in the periphery. It was suggested that the phosphate at C-6 disturbs crystallization [175] and Blennow *et al.* [176] concluded that a major part of this phosphate was associated with the amorphous regions. Later research showed that the phosphate groups also are found in the crystalline parts of the granules [177]. Molecular modelling suggested that C-6 phosphorylation does not disturb the structure of the double helices and their crystal structures [178].

5.6.2 Intermediate branched materials

Intermediate materials are found especially in samples from plants with a modified starch biosynthesis, but were also reported in low amounts in normal starch samples [179–181]. The nature of this material is very different in different samples and thus any clear definition cannot be made. A complicating fact is that the methods for the isolation of intermediate materials differs between laboratories and most certainly affect the results reported. Thus, intermediate material was defined as polymers of intermediate size to amylopectin and amylose [182, 183] and was isolated from the fraction not complexing with 1-butanol (the amylopectin fraction) by GPC [183]. Alternatively, it was isolated as a separate, third fraction from the amylose fraction, which was obtained as a precipitate either in thymol [179] or in a mixture of 1-butanol and isoamyl alcohol [180]. An additional complicating fact is that the structure of the 'normal' amylopectin component in many cases becomes modified. Thus, in *amylose-extender* mutants of maize both the CL of the different categories are longer than normally and the relative amount of long chains increases[183–185]. The *dull-1* mutation possesses a high amount of short chains and thus a high DB [183]. How much the structure of the amylopectin can be allowed to alter before it should be considered as belonging to the 'intermediate' category is certainly impossible to answer.

Maize starches containing increased amylose contents (*amylose-extender* mutants) are best known for their composition of intermediate materials. This intermediate material was reported to have molecular weights intermediate to amylopectin and amylose [180, 183]. It consisted of branched polymers with chains that apparently could be classified as similar to those found in normal amylopectin, but the CL of the chain categories, especially

the long chains, was higher and the ratio of long chains/short chains was high [180, 183, 186–188]. Yuan *et al.* [185] suggested that the category of long chains included long A-chains not found in normal maize starch. Another report characterized the intermediate material as amylose with unusually short chains [189]. It was also reported that the proportion of long chains increased with decrease of molecular weight of the intermediate material [184]. A maize mutant was reported [190] to contain a starch with extremely high apparent amylose content (89.9%). At closer examination, a major part of this 'amylose' was, however, intermediate materials with intermediate molecular weight. The branched material contained unusually much of long chains. 26.5% of the starch was 'amylose' (or linear dextrins) of lower molecular weight than in normal maize starch.

Wrinkled pea starch is a classical example of a starch with increased amylose content. The reported nature of the intermediate material in this starch [191–193] contains all from very short amylose chains mixed with amylopectin with unusually long CL [194] to low molecular weight branched material with sizes corresponding to that of clusters [195] and with a high proportion of long chains [195, 196].

In the endosperm of maize with *sugary-1* mutation a branched, readily water soluble polymer known as phytoglycogen is found in addition to the granular starch. This intermediate material resembles glycogen in its unit chain composition with only a single group of chains [188, 193]. The CL is 10–12 and thus the DB is roughly double compared to normal maize amylopectin [29, 197]. Phytoglycogen is also present in *sugary-1* mutations of rice. The amylopectin component of the starch in these samples was reported to have more of short chains of DP$<$12, but less chains of DP 13–24 compared to the non-mutant starch [198].

6 Locations of molecular components in the starch granule

6.1 The crystalline components

Most common starch granules are much too small to be studied individually by diffraction analysis or solid-state polymer techniques such as spectroscopy. Until recently, there was only a single case where an oriented X-ray diagram had been obtained from an isolated starch granule. This diffraction diagram was obtained in 1951 [199] with an X-ray microcamera from a gigantic grain extracted from the pseudobulb of the orchid *Phajus grandifolius*. This experiment showed that the molecular orientation of the diffracting material was perpendicular to the growth rings of this unusually large granule. The characterization of starch granules, that are elliptical in shape with their long axis never greater than 100 μm, has only become possible in the recent years throughout the use of microfocus X-ray diffraction from SR. X-ray beam of 2 μm full width, having flux of about 10^{10} photons/s/μm^2, as available at European Synchrotron Radiation Facility in Grenoble, France, can be used to map the occurrence of the crystalline regions within a single granule. The granule is not subjected to any sample preparation. Oriented 2D fibre diffraction patterns can be obtained, yielding key information about the nature of the crystalline structure along with its location and orientation with respect to the granule. Diffraction pattern can be collected at 10 μm steps across one single granule, thereby providing a complete mapping of the crystalline components, as schematically represented in Fig. 12. Individual wheat and potato starch granules have been subjected to such an investigation [200, 201]. Individual fibre diffraction patterns,

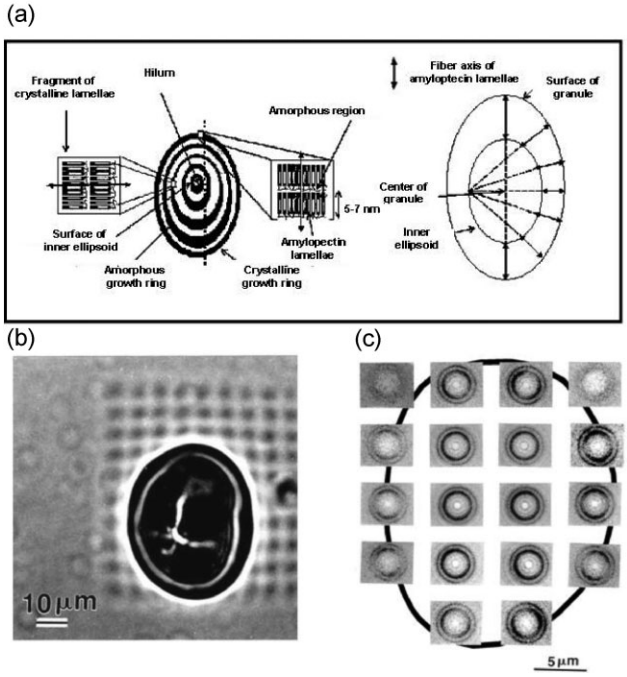

Figure 12. (a) Granule in cross-section showing the orientation of amylopectin double helices in the crystalline lamellae. The dashes line indicates the path followed to obtain the diffraction diagram using a microfocus X-ray diffraction beam having a diameter of 2 μm. (adapted from ref. [201]). Distribution of the crystalline domains in pea starch. (b) Optical micrograph of a typical sample of smooth pea after a 7 μm step irradiation with an X-beam having 2 μm diameter; each step consisting of a 16 s exposure. (c) Set of microfocus X-ray diffraction patterns recorded on a starch granule of smooth pea. Each diagram corresponds to a diffraction area of about 3 μm^2 of the specimen and steps of 7 μm separate the diagrams (from ref. [200]).

having unit cell dimensions in very good agreement with those used for the crystal structure of A- and B-type [89, 90] have been recorded, on cereal and potato individual granules, respectively. Their analysis establishes, without any ambiguity, the orientation of amylopectin double helices in the crystalline lamellae (Fig. 12).

The most accurate mapping has been recorded for potato starch, establishing the orientation of amylopectin double helices in crystalline lamellae. Interestingly, these double helices may be seen not to point towards a single focus, but instead towards the surface of an inner ellipsoid. The helices are radially oriented; *i.e*. they are found to be perpendicular to the surface of the granule. This is in agreement with information derived from birefringence studies, which indicates a similar result although in a less straightforward manner. At the level of 10 μm resolution, there was no discontinuity of orientation (disclination or grain boundaries). This indicates a gradual change in the direction of the helices between 10 μm steps, consistent throughout with radial orientation [201].

The microfocus synchrotron wide-angle diffraction mapping experiments was also used to decipher the crystalline microstructure and the polymorphism of granules from smooth pea, exhibiting the so-called C-type polymorphism [202]. These specimens contain 60% of A-type structure and 40% of B-type structure; and these two crystalline phases co-exist within the same granule.

The A-allomorph is essentially located in the outer part of the granules, whereas the B-type is found mostly in their centre. In the A-component, the diffraction diagrams were always poorly oriented fibre patterns with their fibre axis systematically oriented towards the centre of the granule. In the B-centre of the granule, only powder diagrams could be observed, whereas in middle areas of the granules, the B-component was much better oriented than the A-component. These observations confirm the results of Bograsheva *et al.* [203] who followed the loss of birefringence of the granules during gelatinization in aqueous KCl solution, and found that the smooth pea starch granules had their central part in B-allomorph and their outer part in A-allomorph. They bring a definite answer to the nature of the so-called C-allomorph that is a combination of the A- and B-crystalline constituents. This corroborates previous conclusions derived from molecular modelling whereby the A- and B-arrangements were the only two possible crystalline arrangements of low energy [95]. The synchrotron microbeam used for this investigation had a diameter of around 2 μm. Such a size was small enough to assess the gross ultrastructural features of the diffracting materials of individual starch granules. However, this beam size was still too large to assess the details of the crystalline micromorphology of the individual concentric layers, of about 500 nm in thickness, that are located within the granule. During the scanning of the granule, several of these layers are diffracting at the same time. In the case of starch from smooth pea, it is impossible to assess whether the A- and B-phases are present within the same single layer of the granule or along a single cluster of amylopectin.

The most recent advent of SR machines and the development of the microfocus beamline at ESRF, Grenoble, France [204] have greatly improved the microdiffraction method. The technique has now been applied to a number of starch granules from B and C family [200–202, 205–207] (Fig. 13). X-ray probes with a diameter as low as 0.5 μm are currently available, with the brilliance of the synchrotron and 0.1 μm probes will be available in the near future.

6.2 The supramolecular organization of starch

Even though some detailed information regarding the starch polymer structures has been simulated at the atomic level by computer modelling, the granule structure at the level of the crystalline and amorphous domains (both on the lamella scale and that of the 'growth' rings) is less well understood. Such knowledge is important for an understanding of the physical properties of starch. As stated above, small angle X-ray diffraction and electron microscopy have revealed a periodicity in the granule of about 10 nm which has been explained by stacks of alternating thin crystalline and amorphous lamellae, as proposed in the cluster model of amylopectin [128, 144].

The structural characteristics of the branching point of amylopectin are difficult to assess, however, since they are thought to be located in the amorphous regions between crystallites and since they constitute such a small fraction of the total material. Some basic structural features have, however, been established through computer modelling [208]. In particular, it was found that among the low energy arrangements, the side chains would fold back onto the carrying chain, thereby producing dense 3D structures in which a parallel arrangement is achieved. Furthermore, the branching between two strands of the double helices was investigated. It was found that one particular set of conformations about the glycosidic linkages in the two different strands could result in an arrangement such that double helical strands could be connected through a α-(1–6)-linkage, with a minimum of distortion (Fig. 14). This indicates that the branch points do not induce extensive defects in the double helical structure, but instead may serve to initiate the crystalline arrangement.

The concept of amylopectin forming double helices easily integrates into the currently accepted cluster model, with the short linear chains of the branches being intertwined into double helices, whilst the α-(1–6)-branch points are located in the more amorphous regions between the clusters of double helices. This concept helps in understanding that parts of the amylopectin molecules are capable of forming double helices, which explains the

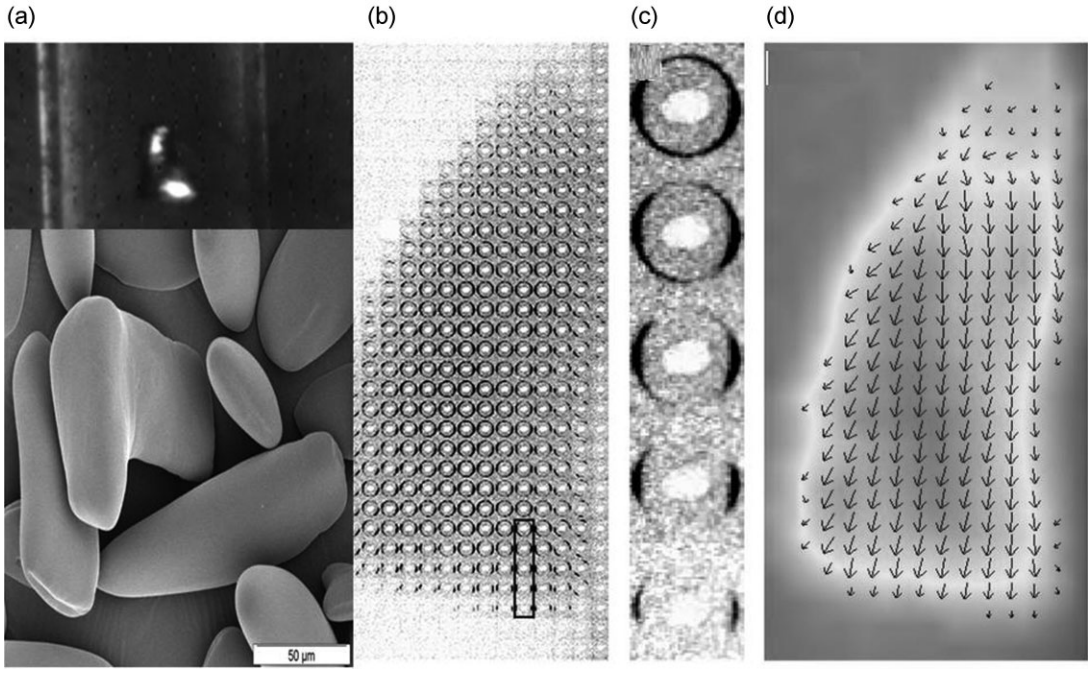

Figure 13. (a) Scanning electron micrograph of a batch of *Phajus grandifolius* starch granules. (b) Composite image composed of X-ray patterns recorded during a mesh scan, showing the outline of an ogival granule inside a glass capillary. (c) Display of five selected diffraction diagrams showing the (1 0 0) reflection ($d = 1.58$ nm); (d) intensity distribution of the crystalline fraction of the granule overlaid with arrows reflecting the orientation of the local fibre axes. The length of the arrows is proportional to local (1 0 0) intensity [205].

apparent anomaly that a branched polymer is the source of structural order within the granule.

According to Hizukuri [105], amylopectin molecules in A-type pattern starches have shorter constitutive chains and more of the short-chain fraction than amylopectin molecules in the B-type starches. Jane *et al*. [209] determined that A-type starches had branch points scattered in both amorphous and crystalline regions, although for its own part, the B-type starch had most branch points clustering in the amorphous ones. It was concluded [209] that the branching pattern of amylopectin played a key role in the determination of the type of crystallinity. Such point of view was confirmed throughout an investigation of the role of the distance between branching points in a cluster related to crystallization pattern of the chain arrangement [23]. The study was performed on two allomorphs, double maize mutants of A- and B-type (*wxdu* and *aewx*, respectively). It was shown that the branching zone of clusters in A-type clusters was larger but with shorter distance between the branching points than in the B-type branching zone of clusters. These results indicate that both CL specificity combined with α-(1–6)-linkage distribution, have to be considered in the cluster feature.

A further interesting observation regarding starch granule molecular order has been gained by solid-state ^{13}C NMR investigation of starch [210]. The ratio of single to double chains in a given starch sample can be assessed. The investigation suggested that the level of helical order is often significantly greater than the extent of crystalline order; which means that starch granules contain double helices moieties, which are not involved in extended crystalline arrays. A novel approach for calculating starch crystallinity and its correlation with double helix content has been developed based on the joint use of X-ray diffraction and solid NMR [211]. The results indicate that a significant proportion of double helices present in starch granules is packed into somehow imperfect crystalline structures. It would therefore appear that this observation is relevant to the amylopectin component of the granule (since amylose is not thought to be extensively in the double helical state); it suggests that much of the amylopectin in the more amorphous shells of the granule is in the double helical form. As mentioned above, computer modelling [208] supports such a view that double helices in amylopectin are sustainable in terms of molecular energetic, even at the α-(1–6) branch points located in the amorphous regions (Fig. 14).

Advances in the field of molecular modelling [212] offer some new possibilities to investigate further the nature and importance of both branch points and amorphous/crystalline interfaces in starch. In approaching these questions, it is wise to adopt the attitude that one is not searching for

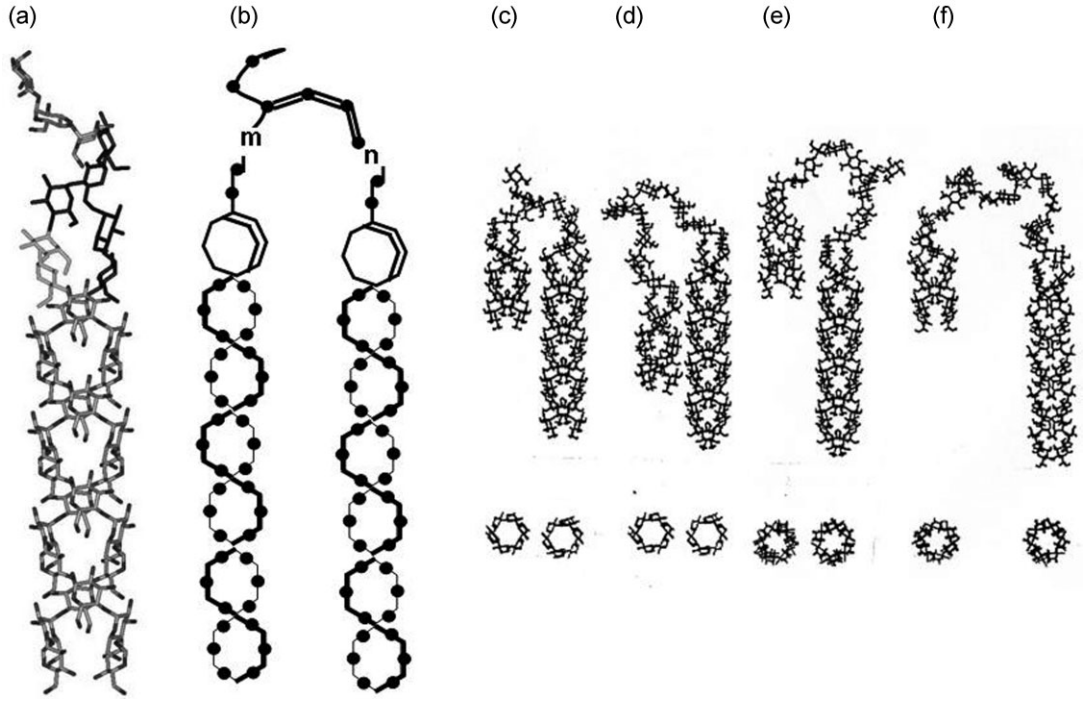

Figure 14. (a) Representation of the double helix of crystalline starch after modelling a branching point between the two strands [208]). (b) Schematic representation showing some parameters underlying the branching between two double helices. The number of α-D-Glc residues on the reducing side and the non-reducing side of the (1–6) linkage are designated as *n* and *m*, respectively. Molecular drawings of some low energy arrangements as a function of *m* and *n*: (c) $m = 1, n = 3$; (d) $m = 4, n = 6$; (e) $m = 6, n = 4$; (f) $m = 7, n = 7$. The $m = 1$ and $n = 3$ model (c) is easily superimposed on two adjacent double helices as found in the A allomorph. The $m = 4$ and $n = 6$ model (d) superimposes equally well on the A and B crystalline starch structures. The $m = 6$, $n = 4$ model (e) corresponds to two non-adjacent double helices of crystalline B starch (from ref. [161]).

single answers, but for all of the indications that would lead to a clearer image of how starch macromolecules are arranged and interact in nature. To this end, subunits of single helices, double helices and branch points were used as building blocks of larger systems [161]. The possible makeup of amylopectin unit clusters was investigated via a series of models, including single–single, double–single and double–double helix systems. The lengths of the single helix section that linked two branch points (internal chains) was systematically varied between values of 0 and 10 glucose residues. It was found that certain ICL lead to parallel double helices. It can therefore, be postulated that the length of internal chains may determine the degree of local crystallinity. Furthermore, it was noted that some of the low-energy arrangements of double helices could be superimposed on either the two adjacent and non-adjacent double helices of crystalline A- and B-starch polymorphs (Fig. 14).

In other instances, the distance between the double helices is so large that it may in fact be a model for branching two amylopectin crystals or unit clusters. The results of such a modelling exercise suggest strongly that the branching in amylopectin does not exhibit a random nature [213]. This, in a sense, is not a surprising feature, as the branching process is essentially under enzymatic control. The location and the length of the branching segments, necessarily reflect the 3D structure and the mechanism of the branching enzymes, along with the spatial and temporal availability of the oligosaccharide complexes involved in the synthesis. It might therefore be emphasized that the characteristics of the branching pattern are as equally important as the CL distribution, playing a determinant role on some physicochemical properties of starch. This work also suggests that chains in the amorphous region may occur in directions different from the main direction of the crystallized chains. Among others, this should explain the flexibility of the amorphous chains during such phenomena as annealing. It may also suggest that the thickness of the amorphous lamellae does not reflect the actual length of the chains in this area, and possibly does not contribute to a certain periodicity in CL.

From all these studies, both experimental and theoretical, some basic structural features may be identified from which much more complex architectures are likely to result.

These features along with their characteristic dimensions are schematically represented in Fig. 15.

It was suggested that the double-helical segments of amylopectin may behave as mesogens in a liquid crystal [162], with double helices forming pairs of external chain segments joined by a branch point. The mesogens could move relative to each other to pack laterally in crystallite regions. Sufficient length of the flexible linker connecting the double-helical mesogen to the polymer would be important for the mesogen mobility. A local concentration of branch points would not be required for the crystallite formation.

The domain structure in starch has been investigated by the combined use of enzymatic hydrolysis followed by either SEM or transmission electron microscopy (TEM), with the aim of characterizing the mosaic composition of starch resulting from the presence of hard and soft material. During α-amylolysis, the most crystalline (hard) regions are less digested than the semi-crystalline (soft) regions (Fig. 16). Examination of the 3D structure of pig pancreatic α-amylase reveals that the binding site cannot accommodate such large and stiff fragments as the double helices found in the crystalline A- and B-allomorph [214].

The susceptibility of starch granules can be quantified following the intensity and the manner by which erosion and corrosion take place. Most of the starch granules are first hydrolysed superficially. Some starches have specific susceptible surface zones, which become pitted due to endocorrosion. As the pits become larger, canals of endocorrosion sink into the granules [8]. Scanning electron microscopy (SEM) observations at high magnification of starch granules, which have been treated by enzymatic hydrolysis, indicates that starch granules are composed of small (50–500 nm diameter), more or less spherical 'blocklets' [8, 215]. These 'blocklet' structures are further discussed with respect to starch granule structure in Section 6.5.

A super helical structure in starch has been suggested from TEM investigation of small, negatively stained granule fragments. Investigating negative staining of crushed lintnerized starch granules, [13] described some 'worm-like ripple structures' in corn starch granules, which were interpreted as 5 nm thick crystalline lamella created by the association of double helices perpendicular to the plane of the lamella. Oostergetel and van Bruggen [216] with a more sophisticated procedure studied lintnerized wheat [15] and potato starch. By combining electron tomography on negatively stained potato starch granule fragments and cryoelectron diffraction of frozen-hydrated granule fragments, a model for the structural organization of amylopectin in potato starch granules has been proposed [216]. The 3D reconstructions of the residual crystallites in potato starch were carried out using negatives taken from a tilt series in the TEM, treated by a low-pass Fourier filter. A helical structure in 3D was observed in stereo mounts, which revealed that the organization of the lamellae was much more complex than was previously thought to be the case. In this model, the helices form a continuous, regular crystalline network, which appears as a skeleton around which the rest of the starch granule is built. The crystalline domains containing the double helical linear segments in the amylopectin macromolecule form a continuous network consisting of left handed helices packed in a tetragonal array. Since neighbouring helices interpenetrate each other, the crystalline lamellae form a more or less continuous super helical structure. Such a semi-crystalline structure is built up from more or less continuous left handed fragments, and has a diameter of approximately 18 nm and a pitch of 10 nm (Fig. 17).

A central cavity within the super helices would have a diameter of about 8 nm. It is proposed that the pitch of the helix in starch originates from the clustering of branch points, and may be characteristic for the botanical source. Helical pitch would therefore be determined directly by the size and organization of the branching enzymes involved in the synthesis of amylopectin.

Independent data have become available from microfocus small angle X-ray scattering (SAXS) experiments performed on potato starch [217]. They corroborate the original super helical arrangement of starch, while adding some interesting details such as the occurrence of two populations of tilted lamellae in the granule that would be present in equal quantities [218].

6.3 The platelet nanocrystals

The results gathered from the various studies presented above, suggest that amylopectin lamellae are involved as components of complex superhelical architecture. The crystalline lamellae are made of parallel arrays of parallel helices having an average thickness of about 7 nm, with some variations depending on the starch botanical source. The lateral dimensions of these lamellae are less characterized. Starch 'micelles' having a diameter of about 15 nm have been reported [219]. The shape and dimensions of the tangential sections of wheat starch granules have been described as hexagonal components with a length of 60 nm and a width of 30 nm [220]. New morphological data on the individual crystalline lamellae of waxy maize starch granules have been reported. By submitting native granules from A-type amylopectin-rich waxy maize to a hydrochloric acid hydrolysis, insoluble residues were obtained [221]. They contained polydispersed platelet nanocrystals that have retained the crystalline A-type of the parent granules. These nanocrystals, that are not totally individualized, have 5–7 nm thickness, and characteristic geometrical features such as 60–65° acute angles; they form parallelepipedal blocks with a length of

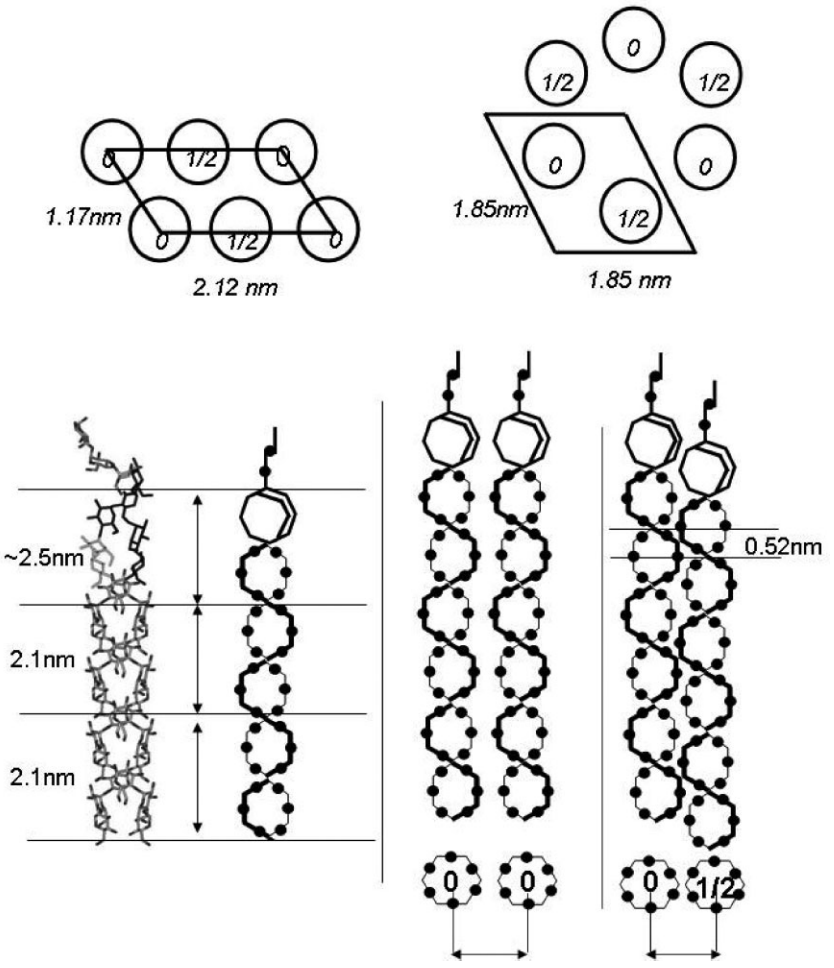

Figure 15. Metrics in Starch: Schematic representations of the unit cell content of A- and B-type 3D structures in their crystalline arrangements. For the A-allomorph, the monoclinic space group is B_2 ($a = 2.124$ nm, $b = 1.172$ nm, $c = 1.069$ nm, $\gamma = 123.5^\circ$), which corresponds to a density of 1.48. For the B-allomorph, the crystalline unit cell is $a = b = 1.85$ nm; $c = 1.04$ nm, $\gamma = 120^\circ$, space group $P6_1$, and the density is 1.41. There is a central channel, which is filled with 36 water molecules, corresponding to a hydration of about 27. From these data, the cross section of double helices can be estimated as 2.1 and 3.0 nm^2, and the volume of paired-double helices as about 15 and 26 nm^3, for the A and B allomorph, respectively. The double helices in both A and B starch are oriented in a parallel fashion; they are left-handed, almost perfectly sixfold structures, with a crystallographic repeating distance of about 1.05 nm, which corresponds to a fibre repeat of 2.10 nm. It is therefore expected that in A type allomorph incorporating two DP 12 single chains intertwined in a double helical fashion will have a length of 4.2 nm (and 6.3 nm in the case of B type allomorph incorporating DP 18 single chains). In both allomorphs, there is a pairing of double helices that corresponds to 1.1 times the distance between the axes of the two double helices. A relative translational shift of 0.5 nm along the orientation of the chains allows a very close nesting of the crests and troughs of the paired double helices. Such a dense association, which is strengthened by O-2...O-6 and O-4...O-3 hydrogen bonding, corresponds to the most energetically favoured interactions between two double helices, thereby generating a duplex of double helices. In the A allomorph, the secondly most energetically favoured interactions are found that corresponds to a translation of 1.17 nm. The parallel helices which form the duplex are labelled 0 and ½ (this indicates their relative orientation along the crystallographic *c* axis). The non-crystalline regions incorporating the 1–6 linkages, extend over a region of about 2.5 nm.

20–40 nm and a width of 15–30 nm. Analysis of the molecular composition showed a major fraction (73% on a molar basis) of dextrins at DP 6–22 (peak DP at 13) that mostly were linear chains. A minor, branched fraction possessed a peak at DP 26 [222].

The molecular composition and the thickness of the lamellae is consistent with the presence of double helical structures made up of single strands having DP between 15 and 18; that would be connected to another chain via α-(1–6)-linkages, in a region that would span about

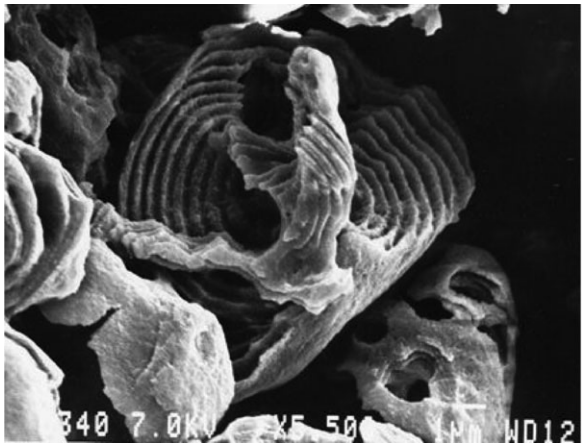

Figure 16. Scanning electron micrograph of waxy maize starch granule after α-amylolysis showing internal canal of corrosion. In the outer shell diameter, the size of the thin canalicles is about 25 nm (D. Dupeyre, CERMAV).

2.5 nm. The crystalline organization of the double helical components would follow the arrangement found in the A-type structure [89]. From the size of the lateral dimensions of the platelets, one can assess that there is a distinct difference between the morphology of the *in vitro* grown crystals [89] and these platelet nanocrystals resulting from concomitant biosynthesis and crystallization.

The overall shape of the starch nanocrystals seems to be a homothetic view of the monoclinic unit cell of the A-type allomorph ($a = 2.12$ nm; $b = 1.17$ nm). The dimensions of the platelets indicate that between 150 and 300 double-helical components are making up the crystalline domains. (Fig. 18). The complementary acute angle of γ angle between the *a* and *b* axes is 56.5°, which is close to the acute angle of around 65° measured for the platelet crystals. Geometrical considerations taking into account the results of the molecular modelling investigations of duplex formation arising from double helical structures can explain the deviation away from the expected morphology of the platelets. They indicate that within the platelets, morphology is driven by the pairing of parallel double helices having their axes separated by 1.1 nm, and a relative translation of 0.52 nm. Such an arrangement allows a very strong nesting of the crests and troughs of the double helices, as it expresses complementary shapes complemented by several inter-double-helices hydrogen bonds [95]. Based on such considerations, the theoretical construction of the nanocrystals 3D-structures, which is in agreement with the crystal structure of A-type starch [89], explains the observed morphology characterized by the acute angle around 65°.

These new findings [222] are therefore very relevant to the nascent morphology of starch assembly, indicating that the double helices are not perpendicular to the observation plane, and that the platelets mean plane is inclined with respect to the axis of the double helices. Therefore, these nanocrystals display two main characteristics, *i.e*. *polarity* (one crystalline face is different from the other one) and *chirality* (resulting from the tilt angle between the double-helical axis and the crystalline axis normal to the base plane). The consequence of these features, which can be also extended to B-type starches, in terms of generating super-helical arrangements should be investigated in the context of the results derived from the analysis of the structure of starch granules with small angle X-ray microfocus scattering [217].

In the native granules the amorphous, branched parts of the amylopectin clusters are additional elements that

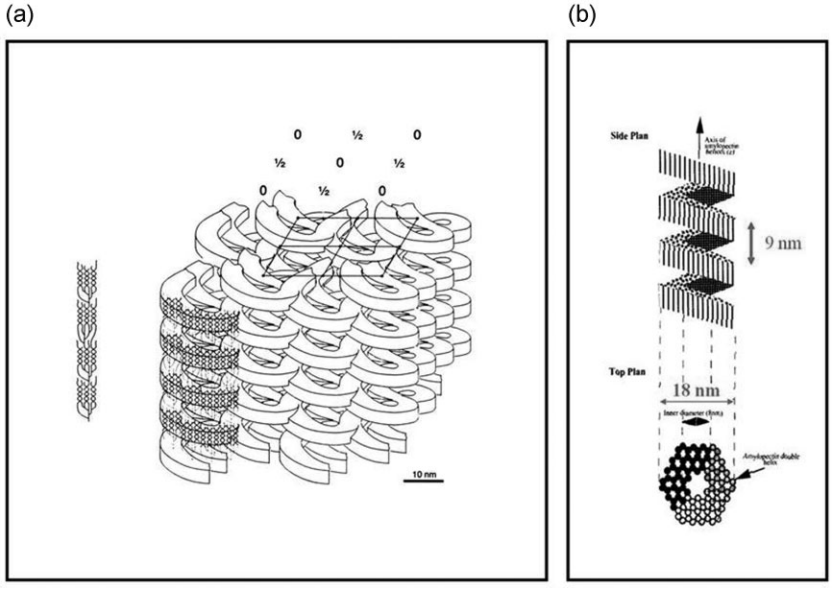

Figure 17. (a) Schematic model for the arrangement of amylopectin in potato starch [15]. The crystalline layers containing the double helical linear segments in the amylopectin molecules form a continuous network consisting of left-handed helices packed in tetragonal arrays. Neighbouring molecules are shifted relative to each other by half of the helical pitch. (b) Additional X-ray studies, using the techniques of small angle and wide angle scattering (SAXS and WAXS) to analyse hydrated starch, show that the lamellae of double helices are probably organized in a helical superstructure, or super helix [218].

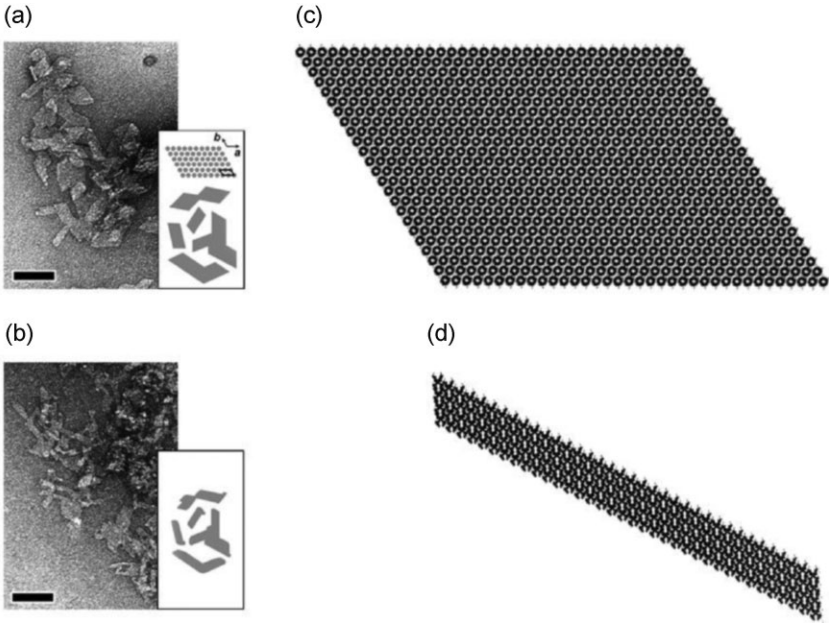

Figure 18. The platelet nanocrystals resulting from: (a) the disruption of wayx maize starch granules by acid hydrolysis (b), followed by a 2 h hydrolysis by α-amylase [222]. Computer representation of an ideal nanocrystal. Schematic representation of the morphology of these crystals showing (c) the composition of the platelet (d) the width of the platelet long with the tilt angle of the double helical components (Courtesy: A. Sarkar & S. Pérez).

participate in the final organization of the crystallites as schematically illustrated in Fig. 19.

6.4 The location and state of amylose within the granule

Until recently, the location and state of amylose within the granule was one of the most important questions, which remained to be elucidated. To date, three main hypotheses for the location of amylose within starch granules have been put forward. The first hypothesis suggested that amylose is laid down tangentially to the radial orientation of the amylopectin, in order to minimize the amylose/amylopectin helical interactions [223]. There is, however, no experimental ground for such a model, which merely considers the need for amylose and amylopectin to have minimal helical interactions. The two other hypotheses advocate radial deposition of the amylose, either in bundles [68, 224] or as individual chains, which are randomly interspersed amongst the amylopectin clusters in both the semi-crystalline and amorphous regions [174, 225]. Of the three hypotheses, the third hypothesis appears to be the most sustainable, since it has been demonstrated, via a cross-linking experiment using maize starch, that amylose chains do not cross-link to one another, but do cross-link to amylopectin chains [174, 225]. In order for this cross-linking of amylose with amylopectin to have occurred, OH-groups from the two chains must have been within 7.5 Å of each other [174]. No cross-linking of amylose chains with other amylose chains was observed, which rules out the second hypothesis that amylose chains occur in bundles. The currently accepted model of amylose location in starch granules is thus as individual, radially

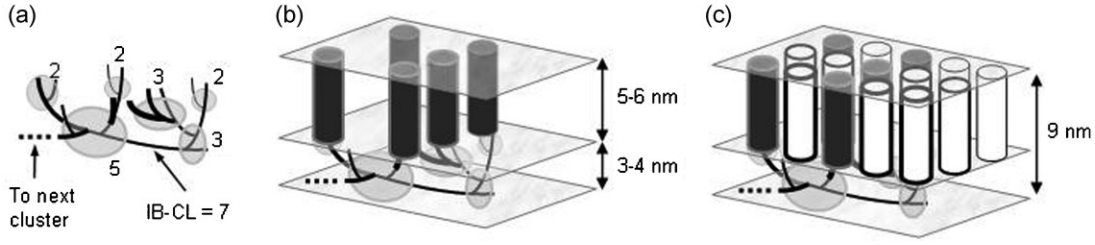

Figure 19. A model of how the clusters of amylopectin build up the semi-crystalline granular rings. (a) 3D illustration of the building block structure of the cluster in Fig. 10. The blocks are attached to a backbone forming a network of chains in the amorphous lamella. Numbers indicate types of building blocks with a corresponding number of chains. IB-CL, inter-block chain length. (b) The same structure with the external chains added forming five double-helices symbolized as dark cylinders in the crystalline lamella. (c) Several hundred double helices from a large number of clusters interact to build up the crystalline lamella.

orientated amylose chains which are randomly distributed amongst the radial amylopectin chains.

There is now substantial evidence indicating that there is an enrichment of amylose towards the periphery of the granule [174, 226–229], and that the amylose found near the surface of the granule has a smaller CL than amylose located nearer the centre of the granule [174]. Consequently, Ring *et al*. [230] demonstrated that the majority of the amylose in the granule could be leached out of granules at temperatures just below the gelatinization temperature. They further demonstrated that the majority of the leached amylose chains were in the single helical state, rather than the double helical state. The single helical state is thus thought to be the predominant state of amylose chains within native starch granules. It is clear, however, from the evidence that amylose can only be completely extracted from granules at temperatures above 90°C [24] that some large amylose molecules are present within the starch granule, and it is further hypothesized that these larger amylose chains which are not easily leached may either participate in double helices with amylopectin [225] or be entangled within the intricate architecture of the starch granule.

In association with the enrichment of amylose towards the granule surface, an enrichment of lipid towards (and at) the granule surface is also believed to exist. Evidence in support of this arises from X-ray microanalysis (EDX) and X-ray photoelectron spectroscopy (XPS) which have demonstrated an enrichment of phosphorous (and hence phospholipids at least) towards and at the granule surface [228, 231, 232]. Furthermore, it is now well established that there is a good correlation between the amylose and lipid contents of all normal (*i.e*. non-mutant) cereal starches [233, 234]. Waxy cereal starches (as well as legume and tuber starches) have small amounts of surface lipids and little or no internal lipids, whilst high amylose cereal starches tend to have more lipid (most of which is internal) than the corresponding normal starch [39]. It is therefore evident that the quantity of lipid in starch granules appears to be linked to the amylose content, and that the lipid appears to be similarly distributed. Furthermore, evidence exists that lipid, like the amylose (and amylopectin) polymers, is aligned radially within the granule [219, 235]. Both the distribution of the lipid molecules in the granule (which is similar to that of amylose) and its probable radial orientation fits well with the evidence that a small proportion of the amylose chains are involved in amylose–lipid complexes. For a long time the evidence for the existence of amylose-lipid complexes in native starch was entirely indirect, arising principally from observations of the conditions required to extract lipids from starches [227, 236] and from the V-type X-ray diffraction pattern which can be observed under the right conditions with native starches. Some evidence for the presence of amylose–lipid complexes in native starches was provided, however, by the use of ^{13}C-cross-polarization/magic-angle spinning nuclear magnetic resonance (^{13}C-CP/MAS NMR) [236].

Using this technique it has thus been demonstrated that amylose–lipid complexes occur in many native cereal starches including wheat, barley, maize, oat and rice. Observation of the amylose content of normal cereal starches (*i.e*. around 25 to 30%) in comparison with the total lipid content (maximum ~1%) suggests however, that only a small proportion of the amylose in such starches is complexed with lipid. Similarly, it is hypothesized that not all of the lipids in starch are involved in amylose–lipid complexes, and that a free-lipid fraction exists [235].

In summary, therefore, substantial information regarding the location and state of amylose has been obtained. Individual amylose chains are believed to be randomly located in a radial fashion among the amylopectin molecules. The concentration of amylose (and lipid) increases towards the surface of the granule, with smaller (leachable) amylose chains predominating near the surface. Amylose chains are believed to be in a single helical state, although a small proportion may be involved in lipid complexes. Some of the larger (non-leachable) amylose chains may be involved in double-helical interactions with amylopectin.

6.5 The blocklet model

The atomic force microscopy (AFM) study by Baldwin *et al.* [237] has allowed the highest resolution images of starch granule surface detail to date to be acquired. These images provide substantial support of earlier SEM observations [1, 11] suggesting that a level of crystalline structure between that of the large 'growth' rings and the amylopectin lamellae exists in starch granules. There is however, substantial other evidence (both from microscopy and non-microscopy techniques) in favour of such a level of granule structure, which has been termed the 'blocklet level of structure' [11]. This section aims to detail this evidence and presents the current reemergence of the 'blocklet' concept.

The idea of crystalline units in starch is not new, and can be originally traced back to the prescience of Nägeli [238], although it was Badenhuizen [239] who first demonstrated the presence of natural resistant units of material in chemically degraded starch. He consequently described these resistant blocks as 'Blökchen Struktur', from which the term 'blocklet concept' is derived. A fibrillar concept of starch granule structure was developed [16, 240] which was viewed as being in opposition to the blocklet concept. The resolution of the microscopes available at the time was not sufficient to solve the debate, and consequently when the ideas leading to the clustering model of amylopectin emerged, the two concepts were largely forgotten. It now

appears, however, that both concepts of granule structure (the blocklet and the fibrillar) were in fact founded in truth, with the fibrillar concept being somewhat related to the radial organization of the amylose and amylopectin polymers, whilst the blocklet concept relates to a higher order of crystalline organization within the granule.

The SEM [1, 11] and AFM [237, 241] images of the blocklet structure provide strong visual evidence of the blocklet structure of starch. A large amount of other supporting evidence from electron microscopy, and enzyme degradation studies exists. Helbert and Chanzy [160], using hydrophilic melamine resin for preparation of ultra thin starch granule sections for TEM, also obtained images in which the outline of individual 'blocklets' with dimensions of a few hundred nanometres can be seen. Such structures have been imaged at higher resolution in sectioned maize starch granules (contrasted with Periodic Acid–Thiosemicarbazide–Silver (PATAg)). The PATAg marker penetrates and thus highlights only the amorphous regions of the granule and has revealed the presence of roughly ellipsoidal regions of 20–500 nm in diameter, which were less easily penetrated by the marker, and which consequently correspond to roughly spherical crystalline 'blocklets' within the granule [11]. Furthermore, the high resolution of the TEM revealed evidence of the alternating crystalline and amorphous amylopectin lamellae within the blocklets [11].

The evidence to date in favour of the 'blocklet' concept of starch granule, therefore indicates that the amylopectin lamellae are organized into effectively spherical 'blocklets' which range in diameter between 20 and 500 nm depending on starch botanical type and their location in the granule. This organization fits with the current knowledge of starch granule structure.

In general, the 'blocklets' are larger (400–500 nm in diameter) in starches of the B- (*e.g*. potato starch) than in starches with the A-crystalline type (*e.g*. wheat starch, in which the 'blocklets' were 25 to 100 nm in diameter). In potato starch however, large 'blocklets' (400–500 nm in diameter) appear to predominate near the granule surface (approximately the outer 10 μm), with smaller blocklets being found nearer the granule centre. In wheat starches, larger (100 nm) 'blocklets' are found in the hard semi-crystalline rings of the granule than in the softer amorphous rings (where blocklet size is around 25 nm). Consequently, it has been hypothesized that whilst granule resistance appears to be linked to several interacting factors, the size of the blocklets (*i.e*. the degree of local crystallinity) may play a role in starch granule resistance [11]. 'Blocklet' size may therefore play a role in the relative resistance of the outer shell of potato starch, and also in the relative resistances of the semi-crystalline and amorphous 'growth' rings (Fig. 20).

Further results in favour of the intermediate 'blocklet level' comes from the work of Atkin *et al.,* [242], who observed small, ellipsoidal particles that were formed during gelatinization of starch granules and released into the surrounding medium if the granules surface was broken. This suggests that the single particles (having dimensions of 400 nm and thus comparable to blocklets) are not covalently linked to each other. It was suggested that a blocklet possibly hosts a single amylopectin molecule [102, 243]. If so, it appears that the blocklet also hosts the super helix and the latter, therefore, represents a single

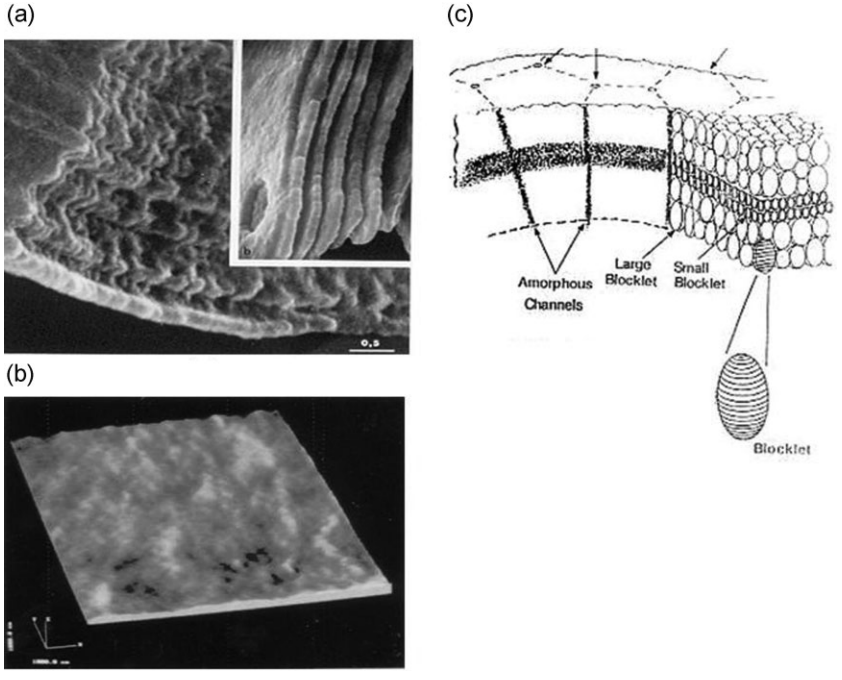

Figure 20. (a) Scanning electron micrographs of starch granules after α-amylolysis showing the occurrence of spherical blocklet-like structures [250]; (b) AFM image of a typical region of the Riband wheat starch granule surface (Scan size 1000 nm^2, *z* height difference of 52.6 nm [250]; (c) Overview of starch granule structure. At the lowest level of granule organization, the alternating crystalline (hard) and semi-crystalline (soft) shells are shown (dark and light). The shells are thinner towards the granule exterior (due to increasing surface area to be added to by constant growth rate). At a higher level of structure, the blocklet structure is shown, in association with amorphous radial channels. Blocklet size is smaller in the semi-crystalline shells than in the crystalline shells [11].

amylopectin macromolecule. Such structure could be formed by turning the backbone of the two-directional cluster model (Fig. 11b–d) into a helix [132]. However, the diameter of the super helix is 18 nm, which is only comparable to the smallest identified blocklets. Larger blocklets should therefore be built up from several helices. Obviously, the relation between the structural levels (blocklets, super helices and amylopectin macromolecules) remains unclear and requires further investigation.

Since the hypothesis of the 'blocklet', as a new structural level, was proposed [11] some information have become available, which have been gathered from different sources of starch. The 'blocklet' appears to be best characterized as an asymmetric structure having an axial ratio of 2 or 3:1, with maximum lengths of about 130–250 nm for pea starch [244], 20–50 nm for potato starch granules [245], as opposed to the 400–500 nm reported by Gallant *et al*., [11], and 10–30 nm for corn starch granules [246]. Despite such differences, some consistent features seem to emerge that have been summarized [247].

(i) The blocklet structure is similar in shape but differs in size according to the plant.
(ii) In the same plant, most of the blocklets are similar in size, although a range of dimensions may occur.

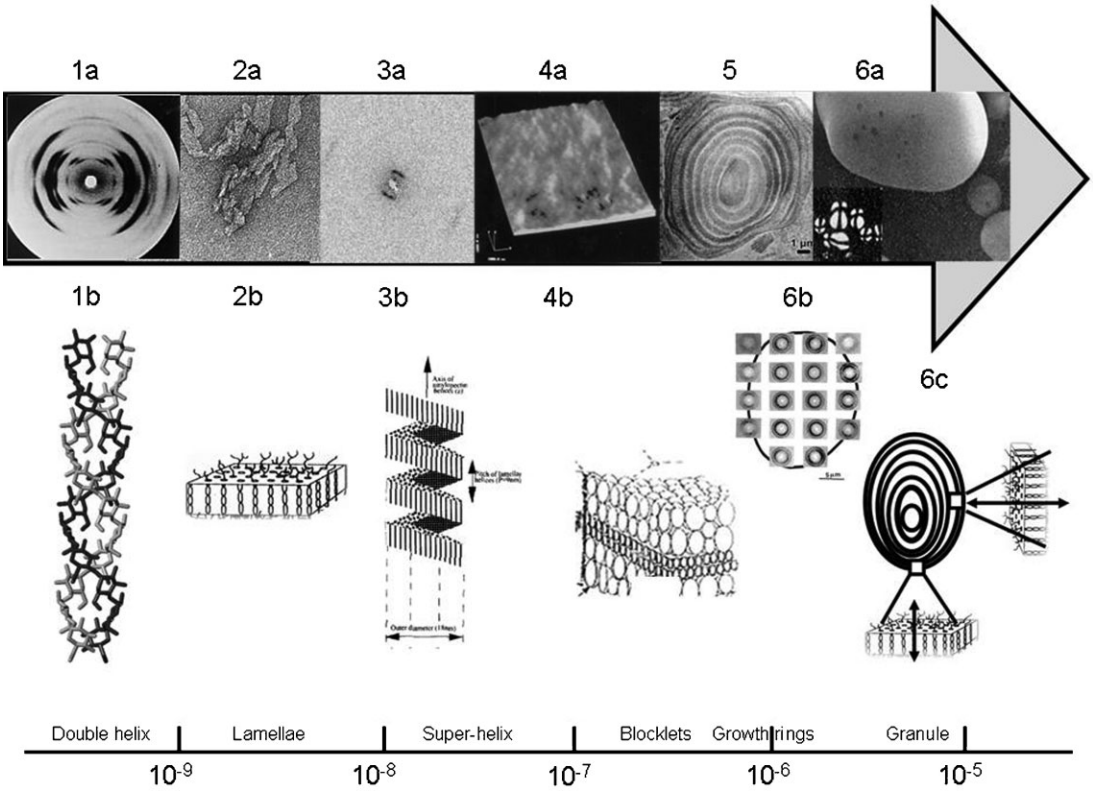

Figure 21. Starch and the powers of ten. The different levels of structural organization spanning five orders of magnitude: From left to right: 1, glucose unit; 1, double helix; 2, lamella; 3, super helix; 4, blocklets; 5, growth rings; 6, granule. (1a) X-ray fibre diffraction pattern demonstrating a double helix structure (Courtesy of A. Imberty *et al.*) (1b) Model of the double helix structure (Courtesy of S. Perez). (2a) Transmission electron microscopy image on hydrolysed starch, showing the shape of the crystalline lamellae (Courtesy of H. Angellier *et al.*) (2b) Model of a crystalline lamella made of about 100 double helices. (3a) Small angle X-ray scattering (SAXS) and Wide-angle X-ray scattering (WAXS) diffraction images indicating the occurrence of a super-helix structure. (Courtesy of Waigh *et al*.) (3b) The super-helix model, with a pitch of 9 nm and a diameter of 18 nm. (4a) Image by atomic force microscopy of a typical surface of a starch granule (Courtesy of D. J. Gallant *et al*.). The bumps seen on the surface show the presence of blocklets. (4b) Blocklet model. The blocklet size is supposed to be smaller in the amorphous regions than in the semi-crystalline regions. Transmission electron microscopy image of an ultrathin section of hydrolysed starch granule showing the growth rings as alternate layers of amorphous and semi-crystalline regions (Courtesy of I. Paintrand, CERMAV). (6a) Starch granule observed by Scanning electron microscopy and the corresponding granule under polarized light. (6b) Set of microfocus X-ray diffraction patterns recorded on a starch granule showing the distribution and orientation of the crystalline domains in a starch granule. Each diffraction pattern corresponds to an area of about 3 μm^2 of the specimen and steps of 7 μm separate two patterns (Courtesy of Buleon *et al*.) (6c) Starch granule section showing the radial orientation of the crystalline domains (lamellae) in a starch granule.

(iii) There is a continuous occurrence of blocklets throughout the granule.
(iv) The blocklet size may not relate to the their granular size, and the thickness of the growth and amorphous rings.
(v) The blocklet assembly may have defects in the amorphous rings and may be assembled loosely.
(vi) An interconnecting matrix surrounding some groups of blocklets may exist.
(vii) The growth rings and amorphous rings are not continuous structures.

Despite the fact that the blocklet has never been extracted and thoroughly characterized from starch granules some general conclusions have been drawn. The blocklet would be a semi-crystalline ultrastructure and, at least in larger blocklets, would generally consist of several amylopectin molecules. A normal blocklet would be constructed by the crystalline and amorphous lamellae that are formed with the clusters of amylopectin molecules. The reducing terminal of amylopectin in the blocklet would be towards the hilum of the granule. Blocklets of two types, *i.e*. 'normal' and 'defects' would be constructed, as the results of the influence of lower branching and non-branching molecules. They would be involved in the formations of heterogeneous and homogeneous shells, respectively.

7 Conclusions

As early as 1858, Carl Nägeli stated '*The starch grain.. opens the door to the establishment of a new discipline .. the molecular mechanics of organized bodies*'. Thus, despite the progress made in understanding starch granule structure, only part of this Pandora's box has been opened, although we are beginning to explore its boundaries. Indeed, with the aid of ever-improving analytical techniques and instrumentation, significant progress has been made in understanding the higher levels of granule orders. The information gathered so far lets us recognize the extreme complexity of the starch granule as a macromolecular assembly. While the whole picture of the starch granule architecture appears better understood, much of the progress reached consists of pieces of information regarding specific features of the granule architecture (Fig. 21). A consistent description of the relationship between these different levels of structural organization is still lacking. It is certainly useful to distinguish between those features which have received widespread acceptance and those which require further investigation.

The following are established features derived from recent applications of instrumentation and methods to the 3D elucidation of complex bio-macromolecules:

(i) Occurrence of segments of amylopectin with a left-handed, parallel-strand double-helical structure.
(ii) Two types of stable arrangement of double helices can occur, as found in the A and B polymorphs.
(iii) Up to 200 double-helical segments are densely packed in platelet nanocrystals, which are polar and chiral.
(iv) The 1–6 branching does not preclude the formation of double helical arrangements.
(v) The 'amorphous' amylopectin may contain a significant amount of double helical components.

An area that remains a focus of investigation is the characterization of a super-helical arrangement of the crystalline lamellae as suggested by some experimental information. Another area of discussion is the occurrence of 'blocklets'. These single particles may be covalently linked to each other and may host a single amylopectin macromolecule. As amylopectin plays a key role in these structures, a thorough understanding of its macromolecular structure is of ultimate importance. The 'cluster' model has been invaluable in helping to decipher the unit chain composition of amylopectin structure via the use of chromatographic techniques in conjunction with enzyme-catalysed digestion. Nevertheless, the organization of the clusters throughout the macromolecule and the organization of the chains within the clusters deserve further investigation. Several alternative modes of organization of the chains exist that are compatible with the features of the granular structures. The influence of amylose, intermediate materials and the minor components on the granular structures are also only partly understood today and remain exciting subjects for further investigations.

The authors have declared no conflict of interest.

8 References

[1] Gallant, D. J., Bouchet, B., Buléon, A., Pérez, S., Physical characteristics of starch granules and susceptibility to enzymatic degradation. *Eur. J. Clin. Nutr.* 1992, *46*, S3–S16.

[2] Hoover, R., Composition, molecular structure, and physicochemical properties of tuber and root starches: A review. *Carbohydr. Polym.* 2001, *45*, 253–267.

[3] Jane, J.-L., Kasemsuwan, T., Leas, S., Zobel, H., Robyt, J. F., Anthology of starch granule morphology by scanning electron microscopy. *Starch/Stärke* 1994, *46*, 121–129.

[4] Srichuwong, S., Sunarti, T. C., Mishima, T., Isono, N., Hisamatsu, M., Starches from different botanical sources I: Contribution of amylopectin fine structure to thermal properties and enzymes digestibility. *Carbohydr. Polym.* 2005, *60*, 529–538.

[5] Tester, R. F., Karkalas, J., Qi, X., Starch-composition, fine structure and architecture. *J. Cereal Chem.* 2004, *39*, 151–165.

[6] Hizukuri, S., Takeda, Y., Yasuda, M., Suzuki, A., Multi-branched nature of amylose and the action of de-branching enzymes. *Carbohydr. Res.* 1981, *94*, 205–213.

[7] Hizukuri, S., Tabata, S., Nikuni, Z., Studies on starch phosphate. Part 1. Estimation of glucose-6-phosphate residues in starch and the presence of other bound phosphate(s). *Starch/Stärke* 1970, *22*, 338–343.

[8] French, D., in: Whistler, R. L., BeMiller, J. N., Pashalls, E. F., (Eds.), *Starch, Chemistry and Technology*, Academic Press, New York 1984, pp. 184–242.

[9] Jane, J.-L., *Starch: Structure and Properties*, CRC Press LLC, Boca Raton, FL 2004.

[10] Gallant, D. J., Bouchet, B. B., Ultrastructure of maize starch granules. A review. *J. Food Microstruct.* 1986, *5*, 141–155.

[11] Gallant, D. J., Bouchet, B., Baldwin, P. M., Microscopy of starch: Evidence of a new level of granule organization. *Carbohydr. Polym.* 1997, *32*, 177–191.

[12] Gallant, D. J., Guilbot, A., Artefacts during preparation of sections of starch-granules. Studies under light and electron microscope. *Starch/Stärke* 1971, *23*, 244–250.

[13] Yamaguchi, M., Kainuma, K., French, D., Electron microscopic observations of waxy maize starch. *J. Ultrastr. Res.* 1979, *69*, 249–261.

[14] Blanshard, J. M. V., Bates, D. R., Muhr, A. H., Worcester, D. L., Higgins, J. S., Small-angle neutron-scattering studies of starch granule structure. *Carbohydr. Polym.* 1984, *4*, 427–442.

[15] Oostergetel, G. T., van Bruggen, E. F. J., On the origin of a low angle spacing in starch. *Starch/Stärke* 1989, *41*, 331–335.

[16] Sterling, C. J., in: Radley, J. A. (Ed.), *Starch and its Derivatives*, 4th Edn., Chapman & Hall, London 1968, pp. 139–167.

[17] McDonald, A. M. L., Stark, J. R., Morrison, W. R., Ellis, R. P., The composition of starch granules from developing barley genotype. *J. Cereal Sci.* 1991, *13*, 93–112.

[18] Buléon, A., Colonna, P., Planchot, V., Ball, S., Starch granules: Structure and biosynthesis. *Int. J. Biol. Macromol.* 1998, *23*, 85–112.

[19] Schoch, T. J., in: Whistler, R. L. (Ed.), *Methods in Carbohydrate Chemistry, IV: Starch*, Academic Press, New York 1964, pp. 25–86.

[20] Chrastil, J., Improved colorimetric determination of amylose in starches or flours. *Carbohydr. Res.* 1987, *159*, 154–158.

[21] Knutson, C. A., Grove, M. J., Rapid method for estimation of amylose in maize starches. *Cereal Chem.* 1994, *71*, 469–471.

[22] Morrison, W. R., Laignelet, B., An improved colorimetric procedure for determining apparent and total amylose in cereal and other starches. *J. Cereal Sci.* 1983, *1*, 9–20.

[23] Gérard, C., Planchot, V., Colonna, P., Bertoft, E., Relationship between branching density and crystalline structure of A- and B-type maize mutant starches. *Carbohydr. Res.* 2000, *326*, 130–144.

[24] Banks, W., Greenwood, C. T., *Starch and Its Components*, Edinburgh University Press, Edinburgh 1975.

[25] Lansky, S., Kooi, M., Schoch, T. J., Properties of the fractions and linear subfractions from various starches. *J. Am. Chem. Soc.* 1949, *71*, 4066–4075.

[26] Gidley, M. J., Bociek, S. M., C-13/MAS NMR studies of amylose inclusion complexes, cyclodextrins, and the amorphous phase of starch granules – relationships between glycosidic linkage conformation and solid-state C-13 chemical shifts. *J. Am. Chem. Soc.* 1988, *110*, 3820–3829.

[27] Boyer, C. D., Simpson, E. K. G., Damewood, P. A., The possible relationship of starch and phytoglycogen in sweet corn. II. The role of branching enzyme I. *Starch/Stärke* 1982, *34*, 81–85.

[28] Doehlert, D. C., Kuo, T. M., Juvik, J. A., Beers, E. P., Duke, S. H., Characteristics of carbohydrate metabolism in sweet corn (sugary-1) endosperms. *J. Am. Soc. Hortical Sci.* 1993, *118*, 661–666.

[29] Inouchi, N., Glover, D. V., Fuwa, H., Chain length distribution of amylopectins of several single mutants and the normal counterpart, and sugary-1 phytoglycogen in maize (*Zea mays* L.). *Starch/Stärke* 1987, *39*, 259–266.

[30] Biliaderis, C. G., Grant, D. R., Vose, J. R., Molecular weight distributions of legume starches by gel chromatography. *Cereal Chem.* 1979, *56*, 475–480.

[31] Goering, K. J., DeHaas, B., A comparison of the properties of large- and small-granule starch isolated from several isogenic lines of barley. *Cereal Chem.* 1974, *51*, 573–578.

[32] Hoh, J. H., Lal, R., John, S. A., Revel, J.-P., Arnsdorf, M. F., *Science* 1991, *253*, 1405–1408.

[33] Yusuph, M., Tester, R. F., Ansell, R., Snape, C. E., Composition and properties of starches extracted from tubers of different potato varieties grown under the same environmental conditions. *Food Chem.* 2003, *82*, 283–289.

[34] Fannon, J. E., Hauber, R. J., BeMiller, J. N., Surface pores of starch granules. *Cereal Chem.* 1992, *69*, 284–288.

[35] Fannon, J. E., Shull, J. M., BeMiller, J. N., Interior channels of starch granules. *Cereal Chem.* 1993, *70*, 611–613.

[36] MacGregor, A. W., Ballance, D. L., Hydrolysis of large and small starch granules from normal and waxy barley cultivars by alpha-amylases from barley malt. *Cereal Chem.* 1980, *57*, 397–402.

[37] Han, X.-Z., Benmoussa, M., Gray, J. A., BeMiller, J. N., Hamaker, B. R., Detection of proteins in starch granule channels. *Cereal Chem.* 2005, *82*, 351–355.

[38] Han, X.-Z., Hamaker, B. R., Location of starch granule-associated proteins revealed by confocal laser scanning microscopy. *J. Cereal Sci.* 2002, *35*, 109–116.

[39] Morrison, W. R., Milligan, T. P., Azudin, M. N., A relationship between the amylose and lipid contents of starches from diploid cereals. *J. Cereal Sci.* 1984, *2*, 257–271.

[40] Morrison, W. R., Starch lipids and how they relate to starch granule structure and functionality. *Cereal Foods World* 1995, *40*, 437–446.

[41] Vasanthan, T., Bhatty, R. S., Physicochemical properties of small- and large-granule starches of way, regular and high-amylose barleys. *Cereal Chem.* 1996, *73*, 199–207.

[42] Lim, S.-T., Kasemsuwan, T., Jane, J. L., Characterization of phosphorus in starch by 31P-nuclear magnetic resonance spectroscopy. *Cereal Chem.* 1994, *71*, 488–493.

[43] Medcalf, D. G., Youngs, V. L., Gilles, K. A., GillesWheat Starches. II. Effect of polar and nonpolar lipid fractions on pasting characteristics. *Cereal Chem.* 1968, *45*.

[44] Jane, J., Kasemsuwan, T., Chen, J. F., Juliano, B. O., Phosphorus in rice and other starches. *Cereal Foods World* 1996, *41*, 827–832.

[45] Lim, S., Seib, P. A., Preparation and pasting properties of wheat and corn starch phosphates. *Cereal Chem.* 1993, *70*, 137–144.

[46] Takeda, Y., Hizukuri, S., Location of phosphate groups in potato amylopectin. *Carbohydr. Res.* 1982, *102*, 321–327.

[47] Takeda, Y., Takeda, C., Mizukami, H., Hanashiro, I., Structures of large, medium and small starch granules of barley grain. *Carbohydr. Polym.* 1999, *38*, 109–114.

[48] Takeda, Y., Shitaozono, T., Hizukuri, S., Molecular structure of corn starch. *Starch/Stärke* 1988, *40*, 51–54.

[49] Shibanuma, K., Takeda, Y., Hizukuri, S., Shibata, S., Molecular structures of some wheat starches. *Carbohydr. Polym.* 1994, *25*, 111–116.

[50] Hizukuri, S., Takagi, T., Estimation of the distribution of molecular weight for amylose by the low-angle laser-light-scattering technique combined with high-performance gel chromatography. *Carbohydr. Res.* 1984, *134*, 1–10.

[51] Takeda, Y., Maruta, N., Hizukuri, S., Examination of the structure of amylose by tritium labelling of the reducing terminal. *Carbohydr. Res.* 1992, *227*, 113–120.

[52] Takeda, Y., Hizukuri, S., Takeda, C., Suzuki, A., Structures of branched molecules of amyloses of various origins, and molecular fractions of branched and unbranched molecules. *Carbohydr. Res.* 1987, *164*, 139–145.

[53] Takeda, Y., Shitaozono, T., Hizukuri, S., Structures of subfractions of corn amylose. *Carbohydr. Res.* 1990, *199*, 207–214.

[54] Takeda, Y., Maruta, N., Hizukuri, S., Structures of amylose subfractions with different molecular sizes. *Carbohydr. Res.* 1992, *226*, 279–285.

[55] Takeda, Y., Hizukuri, S., Juliano, B. O., Structures and amounts of branched molecules in rice amyloses. *Carbohydr. Res.* 1989, *186*, 163–166.

[56] Hayashi, A., Kinoshita, K., Miyake, Y., The conformation of amylase in solution. *Polym. J.* 1981, *13*, 537–541.

[57] Takeo, K., Tokumura, A., Kuge, T., Complexes of starch and its related materials with organic compounds. X. X-ray diffraction of amylose-fatty acid complexes. *Starch/Stärke* 1973, *35*, 357–362.

[58] Katz, J. R., van Itallie, T. B., The physical chemistry of starch and bread making. All varieties of starch have similar retrogradation spectra. *Z. Phys. Chem. Abt.* 1930, *A150*, 90–100.

[59] Zobel, H. F., Starch crystal transformation and their industrial importance. *Starch/Stärke* 1988, *40*, 1–7.

[60] Manley, R. S. J., Chain folding in amylose crystals. *J. Polym. Sci.* 1964, *2*, 4503–4515.

[61] Yamashita, Y., Single crystals of amylose V complexes. *J. Polym. Sci., Part A: Polym. Chem.* 1965, *3*, 3251–3260.

[62] Yamashita, Y., Hirai, N., Single crystals of amylose V complexes. *J. Polym. Sci., Part A: Polym. Chem.* 1966, 161–171.

[63] Yamashita, Y., Monobe, K., Single crystals of amylose V complexes. III. Crystal 81 helical configuration. *J. Polym. Sci., Part A: Polym. Chem.* 1971, *4*, 1471–1481.

[64] Donovan, J. W., Mapes, C. J., Mulitple phase transitions of starch and Nägeli amylodextrins. *Starch/Stärke* 1980, *32*, 190–193.

[65] Kugimiya, M., Donovan, J. W., Wong, T. Y., Phase transitions of amylose-lipid complexes in starches: A calorimetric study. *Starch/Stärke* 1980, *32*, 265–270.

[66] Russell, P. L., Gelatinisation of starches of different amylose/amylopectin content. A study by differential scanning calorimetry. *J. Cereal Sci.* 1987, *6*, 133–145.

[67] Bulpin, P. V., Welsh, E. J., Morris, E. R., Physical characterization of amylose-fatty acid complexes in starch granules and in solution. *Starch/Stärke* 1982, *34*, 335– 339.

[68] Zobel, H. F., in: Alexander, R. J., Zobel, H. F. (Eds.), *Developments in Carbohydrate Chemistry*, American Association of Cereal Chemistry, St. Paul, Minnesota 1992, pp. 1–36.

[69] Morrison, W. R., Tester, R. F., Snape, C. E., Law, R., Gidley, M. J., Swelling and gelatinization of cereal starches. Effects of lipid-complexed amylose and free amylose in waxy and normal barley starches. *Cereal Chem.* 1993, *70*, 385–391.

[70] Godet, M. C., Tran, V., Delage, M. M., Buléon, A., A molecular modelling of the specific interactions involved in the amylose complexation by fatty acids. *Int. J. Biol. Macromol.* 1993, *15*, 11–18.

[71] Goodman, F. O., Garcia, N., Roles of the attractive and repulsive forces in atomic-force microscopy. *Phys. Rev. B* 1991, *43*, 4728–4731.

[72] Leloup, V. M., Colonna, P., Buléon, A., Influence of amylose-amylopectin ratio on gel properties. *J. Cereal Sci.* 1991, *13*, 1–13.

[73] Leloup, V. M., Colonna, P., Ring, S. G., Roberts, K., Wells, B., Microstructure of amylose gels. *Carbohydr. Polym.* 1992, *18*, 189–197.

[74] Miles, M. J., Morris, V. J., Orford, P. D., Ring, S. G., The retrogradation of amylose and amylopectin in the gelation and retrrogradation of starch. *Carbohydr. Res.* 1985, *135*, 271–281.

[75] Miles, M. J., Morris, V. J., Ring, S. G., Some recent observations on the retrogradation of amylose. *Carbohydr. Polym.* 1984, *4*, 73–77.

[76] Miles, M. J., Morris, V. J., Ring, S. G., Gelation of amylose. *Carbohydr. Res.* 1985, *135*, 257–269.

[77] Ring, S. G., Miles, M. J., Morris, V. J., Turner, R., Colonna, P., Spherulitic characterization of short chain amylose. *Int. J. Biol. Macromol.* 1987, *9*, 158–160.

[78] Wild, D. I., Blanshard, J. M. V., The relationship of the crystal structure of amylose polymorph to the structure of starch granule. *Carbohydr. Polym.* 1986, *6*, 121–143.

[79] Gidley, M. J., Bulpin, P. V., Aggregation of amylose in aqueous system – the effect of chain length on phase behaviour and aggregation kinetics. *Carbohydr. Res.* 1987, *161*, 291–300.

[80] Greenwell, P., Evers, A. D., Gough, B. M., Russell, P. L., *J. Cereal Sci.* 1985, *3*, 279–293.

[81] Pfannemuller, B., Influence of chain length of short monodisperse amylose on the formation of A-type and B-type X-ray diffraction patterns. *Int. J. Biol. Macromol.* 1987, *9*, 105–108.

[82] French, A. D., Murphy, V. G., Computer modelling in the study of starch. *Cereal Foods World* 1977, *22*. 61–70.

[83] Gidley, M. J., Molecular mechanism underlying amylose aggregation and gelation. *Macromolecules* 1989, *22*, 351–358.

[84] Zobel, H. F., Molecules to granules. A comprehensive starch review. *Starch/Stärke* 1988, *40*, 44–50.

[85] Pérez, S., in: Kamerling, J. P., Boons, G.-J., Lee, Y. C., Suzuki, A., Taniguchi, N., Voragen, A. G. J. (Eds.), *Comprehensive Glycosciences, B. Analytical Aspects – Scope and Limitations*, Elsevier, Oxford 2007, pp. 347–387.

[86] Wu, H. C. H., Sarko, A., The double-helical molecular structure of A-amylose. *Carbohydr. Res.* 1978, *61*, 27–40.

[87] Wu, H. C. H., Sarko, A., The double-helical molecular structure of B-amylose. *Carbohydr. Res.* 1978, *61*, 7–25.

[88] Buléon, A., Duprat, F., Booy, F. P., Chanzy, H., Single crystals of amylose with a low degree of polymerization. *Carbohydr. Polym.* 1984, *4*, 161–173.

[89] Imberty, A., Chanzy, H., Pérez, S., Buléon, A., Tran, V., The double-helical nature of the crystalline part of A-starch. *J. Mol. Biol.* 1988, *201*, 365–378.

[90] Imberty, A., Pérez, S., A revisit to the 3-D structure of B-type starch. *Biopolymers* 1988, *27*, 1205–1221.

[91] Imberty, A., Pérez, S., Crystal structure and conformational features of alpha-panose. *Carbohdr. Res.* 1988, *181*, 41–45.

[92] Pangborn, W., Langs, D., Pérez, S., A regular left-handed fragment of amylose: The crystal and molecular structure of methyl-alpha-maltotrioside, $4H_2O$. *Int. J. Biol. Macromol.* 1985, *7*, 363–369.

[93] Popov, D., Buléon, A., Burghammer, M., Chanzy, H., *et al*., Crystal Structure of A-amylose: A revisit from synchrotron microdiffraction analysis of single crystals. *Macromolecules* 2009, *42*, 1167–1174.

[94] Imberty, A., Buléon, A., Tran, V., Pérez, S., Recent advances in knowledge of starch structure. *Starch/Stärke* 1991, *43*, 375–384.

[95] Pérez, S., Imberty, A., Scaringe, R. P., in: French, A. D., Brady, J. W. (Eds.), *Computer Modelling of Carbohydrate Molecules*, ACS, Washington, DC 1990, pp. 281–299.

[96] Nishiyama, Y., Putaux, J. L., Montesanti, N., Hazemann, J. L., Rochas, C., B-A allomorphic transition in native starch spherocrystals monitored by in situ synchrotron X-ray diffraction. *Biomacromolecules* 2010, *11*, 76–87.

[97] Aberle, T., Burchard, W., Vorwerg, W., Radosta, S., Conformational contributions of amylose and amylopectin to the structural properties of starches from various sources. *Starch/Stärke* 1994, *46*, 329–335.

[98] Banks, W., Greenwood, C. T., Walker, J. T., Studies on the starches of barley genotypes: The waxy starch. *Starch/Stärke* 1970, *22*, 149–152.

[99] Franco, C. M. L., Wong, K.-S., Yoo, S.-H., Jane, J.-L., Structural and functional characteristics of selected soft wheat starches. *Cereal Chem.* 2002, *79*, 243–248.

[100] Rolland-Sabaté, A., Colonna, P., Mendez-Montealvo, M. G., Planchot, V., Branching features of amylopectins and glycogen determined by asymmetrical flow field flow fractionation coupled with multiangle laser light scattering. *Biomacromolecules* 2007, *8*, 2520–2532.

[101] Yokoyama, W., Renner-Nantz, J. J., Shoemaker, C. F., Starch molecular mass and size by size-exclusion chromatography in DMSO-LiBr coupled with multiple angle laser light scattering. *Cereal Chem.* 1998, *75*, 530–535.

[102] Takeda, Y., Shibahara, S., Hanashiro, I., Examination of the structure of amylopectin molecules by fluorescent labeling. *Carbohydr. Res.* 2003, *338*, 471–475.

[103] Peat, S., Whelan, W. J., Thomas, G. J., Evidence of multiple branching in waxy maize starch. *J. Chem. Soc. Chem. Commun.* 1952, 4546–4548.

[104] Hanashiro, I., Tagawa, M., Shibahara, S., Iwata, K., Takeda, Y., Examination of molar-based distribution of A, B and C chains of amylopectin by fluorescent labeling with 2-aminopyridine. *Carbohydr. Res.* 2002, *337*, 1211–1215.

[105] Hizukuri, S., Relationship between the distribution of the chain length of amylopectin and the crystalline structure of starch granules. *Carbohydr. Res.* 1985, *141*, 295–306.

[106] Bertoft, E., Piyachomkwan, K., Chatakanonda, P., Sriroth, K., Internal unit chain composition in amylopectins. *Carbohydr. Polym.* 2008, *74*, 527–543.

[107] Hizukuri, S., Polymodal distribution of the chain lengths of amylopectins, and its significance. *Carbohydr. Res.* 1986, *147*, 342–347.

[108] Hanashiro, I., Abe, J.-I., Hizukuri, S., A periodic distribution of chain length of amylopectin as revealed by high-performance anion-exchange chromatography. *Carbohydr. Res.* 1996, *283*, 151–159.

[109] Fredriksson, H., Silverio, J., Andersson, R., Eliasson, A.-C., Åman, P., The influence of amylose and amylopectin characteristics on gelatinization and retrogradation properties of different starches. *Carbohydr. Polym.* 1998, *35*, 119–134.

[110] Inouchi, N., Hibiu, H., Li, T., Horibata, T., *et al*., Structure and properties of endosperm starches from cultivated rice of Asia and other countries. *J. Appl. Glycosci.* 2005, *52*, 239–246.

[111] Kong, X., Bertoft, E., Bao, J., Corke, H., Molecular structure of amylopectin from amaranth starch and its effect on physicoshemical properties. *Int. J. Biol. Macromol.* 2008, *43*, 377–382.

[112] Nakamura, Y., Sakurai, A., Inaba, Y., Kimura, I., *et al*., The fine structure of amylopectin in endosperm from Asian cultivated rice can be largely classified into two classes. *Starch/Stärke* 2002, *54*, 117–131.

[113] Singh, N., Singh, S., Isono, N., Noda, T., Singh, A. M., Diversity in amylopectin structure, thermal and pasting properties of starches from wheat varieties/lines. *Int. J. Biol. Macromol.* 2009, *45*, 298–304.

[114] Wang, L., Xie, B., Shi, J., Xue, S., *et al*., Physicochemical properties and structure of starches from Chinese rice cultivars. *Food Hydrocolloids* 2010, *24*, 208–216.

[115] Vandeputte, G. E., Delcour, J. A., From sucrose to starch granule to starch physical behaviour: A focus on rice starch. *Carbohydr. Polym.* 2004, *58*, 245–266.

[116] Genkina, N. K., Wikman, J., Bertoft, E., Yurye, V.P., Effects of structural imperfection on gelatinization characteristics of amylopectin starches with A- and B-type crystallinity. *Biomacromolecules* 2007, *8*, 2329–2335.

[117] Noda, T., Isono, N., Krivandin, A. V., Shatalova, O. V., *et al*., Origin of defects in assembled supramolecular structures of sweet potato starches with different amylopectin chain-length distribution. *Carbohydr. Polym.* 2009, *76*, 400–409.

[118] Bertoft, E., Chains of intermediate lengths in waxy-maize amylopectin. *Carbohydr. Res.* 1991, *212*, 245–251.

[119] Koizumi, K., Fukuda, M., Hizukuri, S., Estimation of the distributions of chain length of amylopectins by high-performance liquid chromatography with pulsed amperometric detection. *J. Chromatogr.* 1991, *585*, 233–238.

[120] Bertoft, E., Lintnerisation of two amylose-free starches of A- and B-crystalline types, respectively. *Starch/Stärke* 2004, *56*, 167–180.

[121] Hanashiro, I., Matsugasako, J.-I., Egashira, T., Takeda, Y., Structural characterization of long unit-chains of amylopectin. *J. Appl. Glycosci.* 2005, *52*, 233–237.

[122] Laohaphatanaleart, K., Piyachomkwan, K., Sriroth, K., Santisopasri, V., Bertoft, E., A study of the internal structure

in cassava and rice amylopectin. *Starch/Stärke* 2009, *61*, 557–569.

[123] Noda, T., Takigawa, S., Matsuura-Endo, C., Kim, S.-J., *et al*., Physicochemical properties and amylopectin structures of large, small, and extremely small potato starch granules. *Carbohydr. Polym.* 2005, *60*, 245–251.

[124] Charoenkul, N., Uttapap, D., Pathipanawat, W., Takeda, Y., Simultaneous determination of amylose content and unit chain distribution of cassava starches by fluorescent labeling/HPSEC. *Carbohydr. Polym.* 2006, *65*, 102–108.

[125] Takeda, Y., Hizukuri, S., Juliano, B. O., Structures of rice amylopectins with low and high affinities for iodine. *Carbohydr. Res.* 1987, *168*, 79–88.

[126] Aoki, N., Umemoto, T., Yoshida, S., Ishii, T., *et al*., Genetic analysis of long chain synthesis in rice amylopectin. *Euphytica* 2006, *151*, 225–234.

[127] Hanashiro, I., Itoh, K., Kuratomi, Y., Yamazaki, M., *et al*., Granule-bound starch synthase I is responsible for biosynthesis of extra-long unit chains of amylopectin in rice. *Plant Cell Physiology* 2008, *49*, 925–933.

[128] Manners, D. J., Recent developments in our understanding of amylopectin structure. *Carbohydr. Polym.* 1989, *11*, 87–112.

[129] Summer, R., French, D., Action of beta-amylase on branched oligosaccharides. *J. Biol. Chem.* 1956, *222*, 469–477.

[130] Walker, G. J., Whelan, W. J., The mechanism of carbohydrase action. 8. Structures of the muscle-phosphorylase limit dextrins of glycogen and amylopectin. *Biochem. J.* 1960, *76*, 264–268.

[131] Bertoft, E., Partial characterization of amylopectin alpha-dextrins. *Carbohydr. Res.* 1989, *189*, 181–193.

[132] Bertoft, E., On the nature of categories of chains in amylopectin and their connection to the super helix model. *Carbohydr. Polym.* 2004, *57*, 211–224.

[133] Yao, Y., Thompson, D. B., Guiltinan, M. J., Maize starch-branching enzyme isoforms and amylopectin structure. In the absence of starch-branching enzyme IIb, the further absence of starch-branching enzyme Ia leads to increased branching. *Plant Physiol.* 2004, *136*, 3515–3523.

[134] French, D., Fine structure of starch and its relationship to the organization of starch granules. *J. Jpn. Soc. Starch Sci.* 1972, *19*, 8–25.

[135] Nikuni, Z., Studies on starch granules. *Starch/Stärke* 1978, *30*, 105–111.

[136] Robin, J. P., Mercier, C., Charbonnière, R., Guilbot, A., Lintnerized starches. Gel filtration and enzymatic studies of insoluble residues from prolonged acid treatment of potato starch. *Cereal Chem.* 1974, *51*, 389–406.

[137] Jacobs, H., Eerlingen, R. C., Rouseu, N., Colonna, P., Delcour, J. A., Acid hydrolysis of native and annealed wheat, potato and pea starches – DSC melting features and chain length distributions of lintnerised starches. *Carbohydr. Res.* 1988, *308*, 359–371.

[138] Jenkins, P. J., Donald, A. M., The effect of acid hydrolysis on native starch granule structure. *Starch/Stärke* 1997, *49*, 262–267.

[139] Kainuma, K., French, D., Naegeli amylodextrin and its relationship to starch granule structure. II. Role of water in crystallization of B-starch. *Biopolymers* 1972, *11*, 2241–2250.

[140] Biliaderis, C. G., Grant, D. R., Vose, J. R., Structural characterization of legume starches. II. Studies on acid-treated starches. *Cereal Chem.* 1981, *58*, 502–507.

[141] Umeki, K., Kainuma, K., Fine structure of Nägeli amylodextrin obtained by acid treatment of defatted waxy-maize starch – structural evidence to support the double-helix hypothesis. *Carbohydr. Res.* 1981, *96*, 143–159.

[142] Watanabe, T., French, D., Structural features of naegeli amylodextrin as indicated by enzymic degradation. *Carbohydr. Res.* 1980, *84*, 115–123.

[143] Bertoft, E., Investigation of the fine structure of alpha-dextrins derived from amylopectin and their relation to the structure of waxy-maize starch. *Carbohydr. Res.* 1991, *212*, 229–244.

[144] Manners, D. J., Matheson, N. K., The fine structure of amylopectin. *Carbohydr. Res.* 1981, *90*, 99–110.

[145] Thurn, A., Burchard, W., Heterogeneity in branching of amylopectin. *Carbohydr. Polym.* 1985, *5*, 441–460.

[146] Bender, H., Siebert, R., Stadler-Szöke, A., Can cyclodextrin glycosyltransferase be useful for the investigation of the fine structure of amylopectins? Characterisation of highly branched clusters isolated from digests with potato and maize starches. *Carbohydr. Res.* 1982, *110*, 245–259.

[147] Finch, P., Sebesta, D. W., The amylase of *Pseudomonas stutzeri* as a probe of the structure of amylopectin. *Carbohydr. Res.* 1992, *227*. c1–c2.

[148] Bertoft, E., Hydrolysis of amylopectin by the alpha-amylase of B. subtilis. *Carbohydr. Res.* 1986, *149*, 379–387.

[149] Bertoft, E., Composition of building blocks in clusters from potato amylopectin. *Carbohydr. Polym.* 2007, *70*, 123–136.

[150] Bertoft, E., Investigation of the fine structure of amylopectin using alpha- and beta-amylase. *Carbohydr. Res.* 1989, *189*, 195–207.

[151] Bertoft, E., Åvall, A-K., Structural analysis on the amylopectin of waxy-barley large starch granules. *J. Inst. Brew.* 1992, *98*, 433–437.

[152] Bertoft, E., Zhu, Q., Andtfolk, H., Jungner, M., Structural heterogeneity in waxy-rice starch. *Carbohydr. Polym.* 1999, *38*, 349–359.

[153] Kong, X., Corke, H., Bertoft, E., Fine structure characterization of amylopectins from grain amaranth starch. *Carbohydr. Res.* 2009, *344*, 1701–1708.

[154] Laohaphatanaleart, K., Piyachomkwan, K., Sriroth, K., Bertoft, E., The fine structure of cassava amylopectin. Part 1: Organization of clusters. *Int. J. Biol. Macromol.* 2010, DOI: 10.1016/j.ibiomac.2010.01.004.

[155] Bertoft, E., Composition of clusters and their arrangement in potato amylopectin. *Carbohydr. Polym.* 2007, *41*, 433–446.

[156] Zhu, Q., Bertoft, E., Composition and structural analysis of alpha-dextrins from potato amylopectin. *Carbohydr. Res.* 1996, *228*, 155–174.

[157] Bertoft, E., Koch, K., Composition of chains in waxy-rice starch and its structural units. *Carbohydr. Polym.* 2000, *31*, 121–132.

[158] Jenkins, P. J., Donald, A. M., The influence of amylose on starch granule structure. *Int. J. Biol. Macromol.* 1995, *17*, 315–321.

[159] Xia, H., Thompson, D. B., Debranching of beta-dextrins to explore branching patterns of amylopectins from three maize genotypes. *Cereal Chem.* 2006, *83*, 668–676.

[160] Helbert, W., Chanzy, H., The ultrastructure of starch from ultrathin sectioning in melamine resin. *Starch/Stärke* 1996, *48*, 185–188.

[161] O'Sullivan, A. C., Pérez, S., The relationship between internal chain length of amylopectin and crystallinity in starch. *Biopolymers* 1999, *50*, 381–390.

[162] Waigh, T. A., Gidley, M. J., Komanshek, B. U., Donald, A. M., The phase transformations in starch during gelatinisation: A liquid crystalline approach. *Carbohydr. Res.* 2000, *328*, 165–176.

[163] Koroteeva, D. A., Kiseleva, V. I., Krivandin, A. V., Shatalova, O. V., *et al*., Structural and thermodynamic properties of rice starches with different genetic background. Part 2. Defectiveness of different supramolecular structures in starch granules. *Int. J. Biol. Macromol.* 2007, *41*, 534–547.

[164] Kozlov, S. S., Blennow, A., Krivandin, A. V., Yuryev, V. P., Structural and thermodynamic properties of starches extracted from GBSS and GWD suppressed potato lines. *Int. J. Biol. Macromol.* 2007, *40*, 449–460.

[165] Kozlov, S. S., Krivandin, A. V., Shatalova, O. V., Noda, T., *et al*., Structure of starches extracted from near-isogenic wheat lines. Part II. Molecular organization of amylopectin clusters. *J. Therm. Anal. Calorim.* 2007, *87*, 575–584.

[166] Lorberth, R., Ritte, G., Willmitzer, L., Kossmann, J., Inhibition of a starch-granule-bound protein leads to modified starch and repression of cold sweetening. *Nat. Biotechnol.* 1998, *16*.

[167] Ritte, G., Lloyd, J. R., Eckermann, N., Rottmann, A., *et al*., The starch-related R1 protein is an alpha-glucan, water dikinase. *Proc. Natl. Acad. Sci.* 2002, *99*, 7166–7171.

[168] Mikkelsen, R., Baunsgaard, L., Blennow, A., Functional characterization of alpha-glucan,water dikinase, the starch phosphorylating enzyme. *Biochem. J.* 2004, *377*, 525–532.

[169] Mikkelsen, R., Blennow, A., Functional domain organization of the potato a-glucan, water dikinase (GWD): Evidence for separate site catalysis as revealed by limited proteolysis and deletion mutants. *Biochem. J.* 2005, *385*, 355–361.

[170] Baunsgaard, L., Lütken, H., Mikkelsen, R., Glaring, M. A., *et al*., A novel isoform of glucan, water dikinase phosphorylates pre-phosphorylated alpha-glucans and is involved in starch degradation in Arabidopsis. *Plant J.* 2005, *41*, 595–605.

[171] Kötting, O., Pusch, K., Tiessen, A., Geigenberger, P., *et al*., Identification of a novel enzyme required for starch metabolism in Arabidopsis leaves. The phosphoglucan, water dikinase. *Plant Physiol.* 2005, *137*, 242–252.

[172] Ritte, G., Heydenreich, M., Mahlow, S., Haebel, S., *et al*., Phosphorylation of C6- and C3-positions of glucosyl residues in starch is catalysed by distinct dikinases. *FEBS Lett.* 2006, *580*, 4872–4876.

[173] Blennow, A., Bay-Smidt, A. M., Wischmann, B., Olsen, C. E., Lindberg-Møller, B., The degree of starch phosphorylation is related to the chain length distribution of the neutral and the phosphorylated chains of amylopectin. *Carbohydr. Res.* 1998, *307*, 45–54.

[174] Jane, J. L., Shen, J. J., Internal structure of the potato starch granule revealed by chemical gelatinization. *Carbohydr. Res.* 1993, *247*, 279–290.

[175] Muhrbeck, P., Svensson, E., Eliasson, A.-C., Effect of the degree of phosphorylation on the crystallinity of native potato starch. *Starch/Stärke* 1991, *43*, 46468.

[176] Blennow, A., Bay-Smidt, A. M., Olsen, C. E., Møller, B. L., The distribution of covalently bound phosphate in the starch granule in relation to starch crystallinity. *Int. J. Biol. Macromol.* 2000, *27*, 211–218.

[177] Blennow, A., Houborg, K., Andersson, R., Bidzinska, E., *et al*., Phosphate positioning and availability in the starch granule matrix as studied by EPR. *Biomacromolecules* 2006, *7*, 965–974.

[178] Engelsen, S. B., Madsen, AÄ., Blennow, A., Motawia, M. S., *et al*., The phosphorylation site in double helical amylopectin as investigated by a combined approach using chemical synthesis, crystallography and molecular modeling. *FEBS Lett.* 2003, *541*, 137–144.

[179] Banks, W., Greenwood, C. T., The fractionation of laboratory-isolated cereal starches using dimethyl sulphoxide. *Starch/Stärke* 1967, *19*, 394–398.

[180] Klucinec, J. D., Thompson, D. B., Fractionation of high-amylose maize starches by differential alcohol precipitation and chromatography of the fractions. *Cereal Chem.* 1998, *75*, 887–896.

[181] Yoon, J.-W., Lim, S.-T., Molecular fractionation of starch by density-gradient ultracentrifugation. *Carbohydr. Res.* 2003, *338*, 611–617.

[182] Gérard, C., Barron, C., Colonna, P., Planchot, V., Amylose determination in genetically modified starches. *Carbohydr. Polym.* 2001, *44*, 19–27.

[183] Wang, Y.-J., White, P., Pollak, L., Jane, J., Amylopectin and intermediate materials in starches from mutant genotypes of the Oh43 inbred line. *Cereal Chem.* 1993, *70*, 521–525.

[184] Takeda, C., Takeda, Y., Hizukuri, S., Structure of the amylopectin fraction of amylomaize. *Carbohydr. Res.* 1993, *246*, 273–281.

[185] Yuan, R. C., Thompson, D. B., Boyer, C. D., Fine structure of amylopectin in relation to gelatinization and retrogradation behavior of maize starches from three wx-containing genotypes in two inbred lines. *Cereal Chem.* 1993, *70*, 81–89.

[186] Baba, T., Arai, Y., Structural characterization of amylopectin and intermediate material in amylomaize starch granules. *Agric. Biol. Chem.* 1984, *48*, 1763–1775.

[187] Boyer, C. D., Liu, K.-C., The interaction of endosperm genotype and genetic background. Part I. Differences in chromatographic profiles of starches from nonmutant and mutant endosperms. *Starch/Stärke* 1985, *37*, 73–79.

[188] Inouchi, N., Glover, D. V., Takaya, T., Fuwa, H., Development changes in fine structure of starches of several endosperm mutants of maize. *Starch/Stärke* 1983, *35*, 371–376.

[189] Adkins, G. K., Greenwood, C. T., Studies on starches of high amylose-content. Part X. An improved method for the fractionation of maize and amylomaize starches by complex formation from aqueous dispersion after pretreatment with methyl sulphoxide. *Carbohydr. Res.* 1969, *11*, 217–224.

[190] Shi, Y.-C., Capitani, T., Trzasko, P., Jeffcoat, R., Molecular structure of a low-amylopectin starch and other high-amylose maize starches. *J. Cereal Sci.* 1998, *27*, 289–299.

[191] Banks, W., Greenwood, C. T., Muir, D. D., Studies on starches of high amylose content. Part 17. A review of current concepts. *Starch/Stärke* 1974, *26*, 289–328.

[192] Biliaderis, C. G., Grant, D. R., Vose, J. R., Structural characterization of legume starches. I. Studies on amylose,

amylopectin, and beta-limit dextrins. *Cereal Chem.* 1981, *58*, 496–502.

[193] Matheson, N. K., A comparison of the structures of the fractions of normal and high-amylose pea-seed starches prepared by precipitation with concanavalin A. *Carbohydr. Res.* 1990, *199*, 195–205.

[194] Boyer, C. D., Damewood, P. A., Matters, G. L., Effect of gene dosage at high amylose loci on properties of the amylopectin fractions of the starches. *Starch/Stärke* 1980, *32*, 217–222.

[195] Bertoft, E., Manelius, R., Qin, Z., Studies on the structure of pea starches. Part 1: Initial stages in alpha-amylolysis of granular smooth pea starch. *Starch/Stärke* 1993, *12*, 215–220.

[196] Colonna, P., Mercier, C., Macromolecular structure of wrinkled- and smooth-pea starch components. *Carbohydr. Res.* 1984, *126*, 233–247.

[197] Yun, S.-H., Matheson, N. K., Structures of the amylopectins of waxy, normal, amylose-extender, and wx:ae genotypes and of the phytoglycogen of maize. *Carbohydr. Res.* 1993, *234*, 307–321.

[198] Wong, K.-S., Kubo, A., Jane, J.-L., Harada, K., *et al*., Structure and properties of amylopectin and phytoglycogen in the endosperm of sugary-1 mutants of rice. *J. Cereal Sci.* 2002, *37*, 139–149.

[199] Kregger, D. R., The configuration and packing of the chain molecules of native starch as derived from X-ray diffraction of part of a single starch grain. *Biochem. Biophys. Acta* 1951, *6*, 406–425.

[200] Buléon, A., Pontoire, B., Riekel, C., Chanzy, H., *et al*., Crystalline ultrastructure of starch granules revealed by synchrotron radiation microdiffraction mapping. *Macromolecules* 1997, *30*, 3952–3954.

[201] Waigh, T. A., Hopkinson, I., Donald, A. M., Butler, M. F., *et al*., Analysis of the native structure of starch granules with X-ray microfocus diffraction. *Macromolecules* 1997, *30*, 3813–3820.

[202] Buleon, A., Gerard, C., Riekel, C., Vuong, R., Chanzy, H., Details of the crystalline ultra-structure of C-starch granules revealed by synchrotron micorfocus mapping. *Macromolecules* 1998, *31*, 6605–6610.

[203] Bogracheva, T. Y., Morris, V. J., Ring, S. G., Hedley, C. L., The granular structure of C-type pea starch and its role in gelatinization. *Biopolymers* 1998, *45*, 323–332.

[204] Riekel, C., New avenues in X-ray microbeam experiments. *Rep. Prog. Phys.* 2000, *63*, 233–235.

[205] Chanzy, H., Putaux, J. L., Dupeyre, D., Davies, R., *et al*., Morphological and structural aspects of the giant starch granules from Phajus grandifolius. *J. Struct. Biol.* 2006, *154*, 100–110.

[206] Lemke, H., Burghammer, M., Flot, D., Rossel, M., Riekel, C., Structural processes during starch granule hydration by synchrotron radiation microdiffraction. *Biomacromolecules* 2004, *5*, 1316–1324.

[207] Riekel, C., Burghammer, M., Flot, D., Rossel, M., Combined micro-drop penetration and microdiffraction for biopolymer hydration experiments. *Fibre Diffr. Rev.* 2004, *12*, 36–40.

[208] Imberty, A., Pérez, S., Conformational analysis and molecular modelling of the branching point of amylopectin. *Int. J. Biol. Macromol.* 1989, *11*, 177–185.

[209] Jane, J. L., Wong, K. S., McPherson, A. E., Branch-structure difference in starches of A and B-type x-ray patterns revealed by their naegeli dextrins. *Carbohydr. Res.* 1997, *300*, 219–227.

[210] Gidley, M. J., Bociek, S. M., Molecular organization in starches: A 13C CP/MAS NMR study. *J. Am. Chem. Soc.* 1985, *107*, 7040–7044.

[211] Lopez-Rubio, A., Flanagan, B. M., Gilbert, E. P., Gidley, M. J., A novel approach for calculating starch crystallinity and its correlation with double helix content: A combined XRD and NMR study. *Biopolymers* 2008, *89*, 761–768.

[212] Pérez, S., in: Kamerling, J. P., Boons, G.-J., Lee, Y. C., Suzuki, A., Taniguchi, N., Voragen, A. G. J. (Eds.), *Comprehensive Glycoscience, B. Analytical Aspects – Scope and Limitation*, Elsevier, 2007, pp. 193–220.

[213] Thompson, D. B., On the non-random nature of amylopectin branching. *Carbohydr. Polym.* 2000, *43*, 223–239.

[214] Casset, F., Imberty, A., Haser, R., Payan, F., Pérez, S., Molecular modelling of the interaction between the catalytic site of pic pancreatic alpha-amylase and amylose fragments. *Eur. J. Biochem.* 1995, *232*, 284–295.

[215] Duprat, F., Gallant, D. J., Guilbot, A., Mercier, C., Robin, J. P., in: Monties, B., (Ed.), *Les polymères Végétaux – Polymères pariétaux et al. mentaires Non Azotés*, Gauthier Villars, Paris 1980, pp. 176–231.

[216] Oostergetel, G. T., van Bruggen, E. F. J., Crystalline domains in potato starch granules are arranged in a helical fashion. *Carbohydr. Polym.* 1993, *21*, 7–12.

[217] Waigh, T. A., Donald, A. M., Heidelbach, F., Riekel, C., Gidley, M. J., Analysis of the native structure of starch granules with small angle X- ray microfocus scattering. *Biopolymers* 1999, *49*, 91–105.

[218] Waigh, T. A., Lisa Kato, K., Donald, A. M., Gidley, M. J., *et al*., Side-Chain Liquid Crystalline Model of Starch. *Starch/Stärke* 2000, *52*, 450–460.

[219] Hizukuri, S., Nikuni, Z., Micelle dimensions of potato starch. *Nature* 1957, *180*, 436.

[220] Kassenbeck, P., Electron-microscope contribution to study of fine-structure of wheat starch. *Starch/Stärke* 1975, *27*, 217–227.

[221] Putaux, J. L., Molina-Boisseau, S., Momaur, T., Dufresne, A., Platelet nanocrystals resulting from the disruption of waxy maize strach granules by acid hydrolysis. *Biomacromolecules* 2003, *4*, 1198–1202.

[222] Angellier-Coussy, H., Putaux, J. L., Molina-Boisseau, S., Dufresne, A., *et al*., The molecular structure of waxy maize starch nanocrystals. *Carbohydr. Res.* 2009, *344*, 1558–1566.

[223] Gidley, M. J., in: Phillips, G. O., Williams, P. A., Wedlock, D. J., (Eds.), *Gums and Stabilizers in the Food Industry*, Oxford University Press, Oxford 1992, pp. 87–92.

[224] Nikuni, Z., Proposed model of starch granule or a starch molecule. *Chori Kagaku (J.)* 1969, *2*, 6–14.

[225] Kasemsuwan, T., Jane, J. L., Location of amylose in normal starch granules.II Location of phosphodiester cross-linking revealed by phosphorous-31 nuclear magnetic resonance. *Cereal Chem.* 1994, *71*, 282–287.

[226] Boyer, C. D., Shannon, J. C., Garwood, D. L., Creech, R. G., Starches of endosperms possessing different alleles at the amylose-extender locus in Zea mays. *Cereal Chem.* 1976, *53*, 327–337.

[227] Morrison, W. R., in: Pomeranz, Y. (Ed.), *Advances in Cereal Science and Technology*, American Association of Cereal Chemists, St. Paul, Minnesota 1978, pp. 224–348.

[228] Morrison, W. R., Gadan, H. J., The amylose content of starch granules in developing wheat endosperm. *J. Cereal Sci.* 1987, *5*, 263–275.

[229] Shannon, J. C., Garwood, D. L., in: Whistler, R. L., BeMiller, J. N., Paschall, E. F. (Eds.), *Starch, Chemistry and Technology*, 2nd Edn. Academic Press, New York 1984, pp. 25–86.

[230] Ring, S. G., L'Anson, K. J., Morris, V. J., Static and dynamic light scattering studies of amylose solutions. *Macromolecules* 1985, *18*, 182–188.

[231] Morrison, W. R., Milligan, T. P., in: Inglett, G. E. (Ed.), *Maize: Recent Progress in Chemistry and Technology*, Academic Press, New York 1982, pp. 1–18.

[232] Russell, P. L., Gough, B. M., Greenwell, P., Fowler, A., Munro, H. S., *J. Cereal Sci.* 1987, *5*, 83–100.

[233] Morrison, W. R., Lipids in cereal starches: A review. *J. Cereal Sci.* 1988, *8*, 1–15.

[234] South, J. B., Morrison, W. R., Nelson, O. E., A relationship between the amylose and lipid contents of starches from various mutants for amylose content in maize. *J. Cereal Sci.* 1991, *14*, 267–278.

[235] Blanshard, J. M. V., in: Gaillard, T. (Ed.), *Starch: Properties and Potential, Critical Reports on Applied Chemistry* Academic Press Ltd., Orlando 1987, pp. 16–54.

[236] Morrison, W. R., Coventry, A. M., Extraction of lipids from cereal starches with hot aqueous alcohols. *Starch/Stärke* 1985, *37*, 83–87.

[237] Baldwin, P. M., Adler, J., Davies, M. C., Melia, C. D., High resolution imaging of starch granule surfaces by atomic force microscopy. *J. Cereal Sci.* 1998, *27*, 255–265.

[238] Nägeli, C. W., Beitage zur näheren Kenntnis des starke grupe. *Annalen der Chemie* 1874, *173*, 218–227.

[239] Badenhuizen, N. P., Die Struktur des Stärkekorns. *Protoplasma* 1937, *28*, 293–326.

[240] Sterling, C. J., Fibrillar structure of starch – Evidence for crossed fibrils from incipient gelatinization. *Starch/Stärke* 1974, *26*, 105–110.

[241] Ohtani, T., Yoshimo, T., Hagiwara, S., Maekawa, T., High-resolution imaging of starch granule structure using atomic force microscopy. *Starch/Stärke* 2000, *52*, 150–153.

[242] Atkin, N. J., Abeysekera, R. M., Cheng, S. L., Robards, A. W., An experimentally-based predictive model for the separation of amylopectin subunits during starch gelatinization. *Carbohydr. Polym.* 1998, *36*, 173–192.

[243] Blennow, A., Bay-Smidt, A. M., Bauer, R., Amylopectin aggregation as a function of starch phosphate content studied by size exclusion chromatography and on-line refractive index and light scattering. *Int. J. Biol. Macromol.* 2001, *28*, 409–420.

[244] Ridout, M. J., Parker, M. L., Hedley, C. L., Bogracheva, T. Y., Morris, V. J., Atomic force microscopy of pea starch granules: Granule architecture of wild-type parent, r and rb single mutants, and the rrb double mutant. *Carbohydr. Res.* 2003, *338*, 2135–2147.

[245] Szymonska, J., Krok, F., Potato starch granule nanostructure studied by high-resolution non-contact AFM. *Int. J. Biol. Macromol.* 2003, *33*, 1–7.

[246] Baker, A. A., Miles, M. J., Helbert, W., Internal structure of the starch resistant granule revealed by AFM. *Carbohydr. Res.* 2001, *330*, 249–256.

[247] Tang, T., Mitsunaga, T., Kawamura, Y., Molecular arrangement in blocklets and starch granule architecture. *Carbohydr. Polym.* 2005.

[248] Buleon, A., Veronese, G., Putaux, J. L., Self-association and crystallization of amylose. *Aust. J. Chem.* 2007, *60*, 706–718.

[249] Imberty, A., Chanzy, H., Pérez, S., Buléon, A., Tran, V., New three-dimensional structure for A-Type Starch. *Macromolecules* 1987, *20*, 2634–2636.

[250] Pérez, S., Baldwin, P. M., Gallant, D. J., in: BeMiller, J. N., Whistler, R. (Eds.), *Starch, Chemistry and Technology*, Academic Press, Elsevier 2009, pp. 149–192.

